FINAL REPORT ON F.I.R.T.A. PROJECT

"Tide and Current Analysis in the Gulf of Carpentaria and its Relation to Banana Prawn Larval Dispersion"

Staff Participating in the Project

Dr J.A. Church	Research Scientist	CSIRO Marine Laboratories Division of Oceanography P.O. Box 21, Cronulla, NSW 2230
Mr A.M.F. Forbes	Experimental Officer	CSIRO Marine Laboratories Division of Oceanography P.O. Box 21, Cronulla, NSW 2230
Dr P. Rothlisberg	Research Scientist	CSIRO Marine Laboratories Division of Fisheries Research P.O. Box 120, Cleveland, Q 4163

Dr J.A. Church
CSIRO Marine Laboratories, Division of Oceanography
P.O. Box 21, Cronulla, NSW 2230

8 November 1981

78/36 Tide and current analysis in the Gulf of Carpentaria and its relation to banana prawn larval dispersion.

CSIRO. Division of Fisheries Research and Oceanography.

- This project is a superb example of a multi-disciplinary approach.

- It ties in the results of the oceanographic study with knowledge of banana prawn larval development and behaviour. The results contribute significantly to our understanding of banana prawn recruitment in the Gulf of Carpentaria.

- The detailed oceanographic knowledge can also be very useful for other purposes too, such as studying tiger prawn recruitment, or assessing a proposal to dump coal ash in the Gulf.

- The objectives of the project have been achieved, and positive results obtained.

- The methodology used has proven successful and the results are already contributing to the ability of scientists to predict banana prawn seasons.

- No doubt results will in the long term also assist in prediction of tiger prawn catches.

- Some further research is needed in order to find a closer correlation of water movements with recruitment.

- CSIRO should continue this work. They are a competent organization who should be supported in future.

- The full report should be produced as a CSIRO publication and a summary prepared for "Aust. Fish.". Some aspects have already been published in scientific journals.

- The project was comparatively cheap, and has produced good value for money.

- The researchers should be commended.

8369y

Summary

The prawn fishing industry in the Gulf of Carpentaria is worth $100 million/year and a large proportion of this is from catches of banana prawns (*Penaeus merguiensis*). In one stage of their complex life history, banana prawn larvae are carried by ocean currents from their spawning grounds to the estuarine nursery areas. The aim of this project was to define the currents that carry the larvae so that the life history can be more fully understood and various biological hypothesis concerning the banana prawn and in particular the behaviour of larvae can be fully tested. To achieve these goals a mixture of field work and theoretical modelling and cooperation between physical oceanographers and fisheries biologists was required.

Self recording current meters were deployed in the south-eastern corner of the Gulf to determine the tidal currents in this area. Satellite-tracked buoys were deployed in the centre of the Gulf to determine the large scale circulation. These data, together with historical tide and meterorological data around the coast, were used to develop a two-dimensional computer model of the tidal and seasonal circulation patterns. There was excellent agreement between the results of these models and the available observations.

This two-dimensional model was extended to three-dimensions and the currents evaluated with this model used to predict the horizontal movement of larvae which migrate vertically through the water column on a day-night cycle. The results indicate the timing and location of spawning is important if tidal currents are to transport the larvae towards the estuarine nursery areas. In the south-east corner of the Gulf (the centre of the banana prawn fishery), the larvae from the October spawning are carried by the tidal currents towards the estuary and thence go to form the March fishing stock; whereas the larvae from the March spawning are carried away from the estuaries and are hence lost to the fishery.

Introduction

The prawn fishing industry in the Gulf of Carpentaria (hereafter referred to as the Gulf) is worth $100 million/year and a large proportion of this is banana prawn (*Penaeus merguiensis*). In one stage of their complex life history, banana prawn larvae are carried by ocean currents from the spawning grounds to the estuarine nursery areas. Our ultimate goal in this project was to be able to understand the various mechanisms which control the movement of the banana prawn larvae.

Our approach was to use the available historical data and data from field work conducted during the program to support mathematical (computer) models. The first model developed was a two-dimensional non-linear model which evaluates the sea surface elevation, and the depth-averaged currents for typical tidal conditions as a function of time and position. The residual circulation (i.e. that part of the current remaining after removal of the tides) was then investigated. Since it was found that banana prawn larvae move vertically through the water column (Rothlisberg in press) on a diurnal cycle, it was necessary to extend the two-dimensional model to three-dimensions for direct computation of the movement of the larvae.

In this report, we first present the biological and physical background to the study, then discuss the methods used, present the results and then finally discuss some of the results. The scientific papers which have resulted from the work are attached as an appendix and they contain details of the work some of which are not included in the main report.

Biological Background

The physical and biological factors affecting larval survival have long been recognised as playing a large part in establishing year class strength in virtually all commercial fisheries around the world. Most of the studies, to date, however, have either been descriptive or correlative with little knowledge of mechanisms that affect larval survival or distribution. The larval ecology of penaeid prawns is no exception. Several hypotheses (for review see Garcia and Le Reste 1981) about how larvae and postlarvae are moved from offshore spawning grounds to nearshore or estuarine nursery grounds , have been put forward with very little understanding of the underlying physical and biological mechanisms.

In Australia there were two pertinent biological studies that addressed the problem of postlarval recruitment. The first was a study by Penn (1975) that suggested a relationship between the vertical distribution of penaeid larvae and the interaction with seasonal tidal currents in Shark Bay, Western Australia. The untested hypothesis was based on incomplete knowledge of larval vertical migratory behaviour and incomplete knowledge of the seasonal current regimes in the area. The other study of relevance was that of Staples (1979, 1980) who studied recruitment patterns of the postlarvae of the banana prawn, *Penaeus merguiensis*, in the Gulf of Carpentaria. He found temporal and spatial trends in postlarval recruitment that could not be explained by adult distribution and reproductive activity alone. He too had incomplete knowledge of current regimes but hypothesized that "The differences in the seasonal pattern of immigration of postlarvae in different areas of the Gulf of Carpentaria arise from both geographical and yearly differences in the fate of larvae produced during these two spawning seasons. The life cycle in the north is dominated by the survival through to juveniles of the March-April larvae, whereas the cycle in the south is dominated by the survival of the September-October larvae.". From these two

studies it became apparent that a detailed understanding of both larval behaviour and current regimes would be necessary to understand the mechanism behind larval movements from the offshore spawning grounds to the nearshore nursery grounds, and thereby help explain not only the seasonal and spatial patterns in postlarval immigration but also the year to year variation in recruitment strength to the juvenile populations and the subsequent adult stocks. Starting in 1976, as part of the Larval Ecology Project of the Tropical Prawn Project of CSIRO, repeated discrete-depth sampling of penaeid larvae, at two locations in the Gulf of Carpentaria was undertaken. The results of this study (Rothlisberg, in press) showed that the variable vertical migratory patterns of larvae depend on stage of development of the larvae and light penetration.

Physical Background

Early studies of the hydrological conditions in the Gulf were completed by Rochford (1966) and Newell (1973). During the winter months convective overturn ensures well-mixed conditions. From late September until March, a seasonal thermocline with vertical temperature difference of up to 5°C exists in water deeper than 30 m. While large scale baroclinic motions were inferred from hydrological observations by Newell (1973), it is expected that with the large tidal range (up to 2 m) and the shallowness of the Gulf, barotropic tide and wind-induced currents are larger than the baroclinic motions. Direct current measurements at four locations in the Gulf (Cresswell 1971) revealed tidal currents up to 0.75 m s^{-1} and non-tidal currents of only 0.08 m s^{-1}.

Easton (1970) used the tidal constants from a number of locations in the Gulf to draw co-tidal and co-range charts for the M_2 and K_1 constituents. The co-range charts indicate that the M_2 amplitude varies from 1 m on the south coast of Irian Jaya to less than 0.30 m at Karumba,

and the K_1 amplitude varies from less than 0.30 m in the north to 1 m at Karumba. On the M_2 co-tidal chart, an amphidromic point is shown just to the west of Torres Strait and on the K_1 co-tidal chart an amphidromic point is shown midway between the northern extremity of Cape York and Cape Arnhem. Due to lack of information, these charts are not detailed and Easton (1970) states that for the M_2 constituent "further nodal points occur probably near Karumba and Groote Eylandt".

By treating the Gulf as a resonator on a semi-infinite channel, Williams (1972) and Buchwald and Williams (1975) investigated the tidal dynamics. Williams (1972) found that the Gulf should have resonances at periods of 7.9 h, 10.4 h and 16 h and that the response at Karumba to an incoming semi-diurnal tide should be very small. Melville and Buchwald (1976) suggested that the magnitude of the ter-diurnal tidal components in the Gulf may be due to the resonance at 7.9 h predicted by Willaims (1972) or to shallow water effects. From analysis of sea level residuals (after removal of tidal components), Melville and Buchwald (1976) found resonant oscillations at periods of 10.6 h and 16 h in agreement with the work of Williams (1972). It was suggested that further activity found at periods of 30-40 h may be associated with disturbances in the Indian Ocean and Coral Sea. Rienecker (1979) extended the work of Williams (1972) to include frictional losses and developed two depth-integrated numerical models.

During the course of this work, Webb (1981) completed the development of a linear numerical model of the Gulf/Arafura Sea system. This model extends the analytical work of Williams (1972) to include friction, curved boundaries and variable bottom topography as well as including the Arafura Sea.

Methods

Current Meter Observations

While there is a large amount of tide height data available on the coast, there are few observations of currents. The few measurements available Cresswell (1971) are of only a few (1 to 8) days duration and it is thus not possible to accurately determine the tidal or residual currents from this data. Because the main interest was centred in the south-east corner of the Gulf, we restricted direct current meter measurements to this area.

Aanderaa (RCM4) current meters were deployed with the common U-type mooring at three locations in the south-east corner of the Gulf (Fig. 1). The three moorings were in depths between 17 and 20 m. Each mooring consisted of two current meters suspended by two subsurface torpedo shaped floats. The top meter was 11 m above the bottom and the lower meter 6 m above the bottom. Ten or fifteen minute sampling intervals were used on all meters. The moorings were first deployed in mid September 1978 from the F.R.V. 'Judy B'. It was originally planned to have continuous records from this time until the start of the banana prawn fishing season in March 1979, however, a combination of heavy marine fouling in the shallow tropical waters, trawling up of the meters by fishermen, and difficulties in servicing the moorings at regular intervals resulted in only three months of useful records being obtained. Because of the problems associated with measuring small residual currents in the presence of strong tidal signals the compasses of the current meters were carefully calibrated. Throughout the period when the moorings were deployed, the difference in temperature recorded by the two meters on each mooring was less than 0.5^{o}C. Hydrological information in the vicinity of the mooring generally indicated vertical temperature differences of 1^{o}C or less although on some occasions near mooring 1, vertical temperature differences as large as 6^{o}C were observed.

Twice daily wind measurements (0900 h and 1500 h) were available from the Bureau of Meteorology station on Mornington Island for the period when the current meters were deployed. This station was thought to give the most representative wind information of any of the coastal stations in the south-east corner. Unfortunately there were a number of gaps in the wind records.

Satellite-tracked Buoy Studies

Satellite-tracked drogued buoys were also released in the Gulf. These buoys are tracked by a NASA (National Aeronautics and Space Administration, U.S.A.) meteorological satellite, NIMBUS-VI. Although there are usually two fixes per day, with r.m.s. position errors of 5 km, the NIMBUS-VI satellite is being phased out and in the present study, time between fixes was often 3 days. This was not a major problem because of the slow movement of the buoys. The buoys were drogued at 20 m depth with a 4.5 m radius parachute.

Computer Models

To extend our knowledge of the tidal currents from the measurements in the south-eastern corner of the rest of the Gulf, it is both convenient and economical to simulate the circulation using a numerical model. This is a computer model which divides the Gulf into a grid formed by the intersection of a series of north-south, east-west lines, 15 n miles apart. Calculations are then made by the computer at each grid point. Along a line joining the Wessel Islands to False Cape in Irian Jaya the tidal height and phase (a measure of the time of arrival of the maximum height) are specified, and the model then allows the tide to propagate from this "open boundary" over the rest of the grid points which represent the Gulf. Calculations are made repetitively over all grid points to derive tidal current velocity from tide heights, and these hourly values are printed out. The numerical model is run for periods simulating up to 29 days in real time.

The results of the model run are then compared with observations of tide heights at ten stations around the Gulf, and with observations of tidal currents at the three mooring locations in the south-eastern corner. After a series of such computer model runs, each containing adjustments of the tide at the open boundary, an accurate model of the tide and tidal currents was derived.

The tidal currents produced by the model are depth averaged values. For this model to be accurate there should be little change of current direction with depth and the near bottom current should be simply related to the depth averaged current. Our current meter records show that there is very little change in direction of the current with depth and that near bottom current speeds are about 85% of mid depth speeds. In the Gulf, temperature and density are fairly constant between the surface and the bottom (as assumed in the model) for the major part of the year and only in summer is there a warm surface layer which may tend to move independently of the lower layer. The tidal currents, which both the model and the observations show as dominating the Gulf circulation, are strong enough in some coastal areas (notably the south-east corner and the northern region along the coast of Irian Jaya) to mix the water column, and in other, deeper water areas, wind can mix the water column from surface to bottom. These factors support the use of a depth averaged numerical model of the circulation.

Torres Strait connects the north-eastern Gulf to the Coral Sea but the volume of water transported into the Gulf through the Strait is very small in comparison with the flow from the Arafura Sea. At this boundary, the numerical model uses a tidal flow rather than using tide heights.

The model was also used to investigate the residual currents (i.e. that part of the currents remaining after the tidal signal was removed) generated by non-linear effects associated with the tide, and surface wind stress.

For this application, the numerical model was run for 15 days (covering a spring-neap cycle) and the hourly output of tidal currents filtered to produce residual currents. Analysis of ten years of monthly wind frequency data for 10 Bureau of Meteorology stations around the Gulf (Fig. 1) shows that there is a smooth annual variation in amplitude from south-east trades (which peak in July) to north-west monsoons (which peak in January). The wind induced currents were modelled by calculating a mean wind stress (which is proportional to the square of the wind speed) for each month at each station and from these data producing a smoothed grid of wind stress for the whole Gulf which was then applied in the model.

As indicated above this model produces depth averaged currents. Frictional effects at the surface (due to wind stress) and at the bottom due to bottom friction lead to significant departures of the current from its depth averaged value. To extend the results of the two-dimensional model to three-dimensions we used a technique first developed by Jelesnianski (1970). In this approach; the currents are driven by the sea surface slope (determined from the two-dimensional model) surface wind stress and bottom friction. The currents as a function of depth below the surface can then be derived using empeirical data for the vertical viscosity and an analytical solution due to Jordon and Baker (1980). The full details of this method are given in a paper presently in preparation.

After heavy monsoon rains, the salinity of waters in the coastal regions (normally 35‰) of the Gulf can be as low as 20‰ due to dilution by freshwater runoff. This low salinity water is lighter than the saline Gulf water resulting in a strong offshore density gradient. This gradient produces offshore currents at the surface, longshore currents at mid depth and onshore currents at the bottom. An analytical method developed by Heaps (1972) was used to model these currents in the Gulf.

It considers the balance between the pressure gradient (due to the increasing density offshore) frictional shear stress and the effect of the rotation of the earth (which deflects the current to the left). Heaps' method of calculating the resulting density currents assumes vertically well-mixed conditions with density contours parallel to the coast.

Movement of Larvae

Finally, the results of the mathematical models were used with the available biological data on the vertical migration of larvae to compute the horizontal transport of these larvae by the tidal and non-tidal currents.

The simplest procedure used was to assume that the larvae remained at one level (i.e. near surface, mid-depth or near bottom) throughout the day/night cycle. A more realistic scheme is for the larvae to move vertically through the water column coming closer to the surface at night and returning to the bottom layers during the day. The larvae were considered to move through the entire water column or only a small fraction of the water column and the extent of the vertical migration was taken as dependent on the age of the larvae.

The currents used for the horizontal transport were computed with the two-dimensional model (or the equivalent three-dimensional model) for a 20-day period commencing on 16 March 1978 and another period commencing on 10 October 1978. These two periods correspond to the two peak spawning periods for banana prawns in the Gulf.

Results

Current Meter Observations

The raw current meter data was smoothed with a low pass filter to produce hourly values.

The tidal signal was then isolated by filtering the hourly values with Munk's "tide-killer" filter (half power response at 0.32 cycles per day) and subtracting the resultant signal from the original series. The tidal signal accounted for more than 90% of the variance of each time series (Table 1). Tidal constants, H and g, (g(-10): Greenwich phase lag for time zone - 10 h), were derived from the time series using a set of programs (based on the least squares method) described by Easton (1977). The most important constituents in each tidal band were included in this analysis. Because there was not enough data to separate the K_1 and P_1 tidal constituents, the estimated K_1 tidal constituent from each analysis was split into the "true" K_1 and the satellite P_1 tidal constituents using the ratio and phase lag difference of the K_1 and P_1 constituents at Karumba. This ratio (P_1/K_1) was 0.27 and the phase lag difference ($g_{K_1}-g_{P_1}$) was 3.2^{o}. In the south-east Gulf, the S_1 constituent ($15.000\ {}^{0}h^{-1}$) is more probably due to local meteorological forcing than to the solar gravitational attraction. Since this local forcing will be quite variable, no attempt was made to determine the constants for the S_1 constituent. Also, no attempt was made to "split" the constituents in the higher frequency tide bands.

These tidal constants were used to construct a "predicted" tidal signal which was subtracted from the observed tidal signal to leave the residual currents. The percentage variance of the signal in the tidal bands unaccounted for by the analysis is given in Table 1. This residual variance is due to the presence of undetermined tidal constituents and also the presence of a non-tidal continuum in the spectrum at tidal frequencies. The tidal constants (with error estimates) for the two principal diurnal components O_1, K_1, and the two principal semi-diurnal components M_2, S_2 (corrected for the effects of the filters used) for the northward and eastward component of each time series, are given in

Table 2. The major and minor axis for the tidal ellipses for the K_1 and M_2 constituents are given in Fig. 2. In all cases except one, the currents rotate clockwise at each location. For the second and third moorings, the major axis of current ellipses for the meter closer to the bottom are rotated anticlockwise relative to the major axis of the top meter (i.e. the opposite direction to that expected for Ekman veering in the southern hemisphere) by several degrees.

Rotary spectral techniques were used to analyse the residual currents. The spectra are qualitatively similar at all locations and shows energy levels rising at low frequencies and also peaking in the tidal bands. These peaks are however much smaller (a factor of 100 in the diurnal band) than in the spectra of the original data. The peaks in the tidal bands may be due to non-linear tide and tide surge interaction and the inability to determine all of the tidal constants with the limited velocity data available.

Stick plots of the data after filtering with Munk's low pass "tide-killer" filter and decimating to 12-hourly values are shown in Fig. 3 and the mean currents from the complete series are given in Table 1. The currents from the two meters on each mooring appear to be highly correlated. For low frequencies (less than 2/3 cycles per day), cross rotary coherence between meters on the same mooring is high ($c^2 \approx 0.8$) and the phase difference is approximately zero for both positive and negative frequencies. Cross rotary coherences between currents from meters on different moorings were evaluated using the longer series at each mooring. In the low frequency band, the coherences just reach the 95% level. The current components were regressed against the wind components. For this regression, the 0900 h and 1500 h wind readings were averaged and the 1200 h low passed currents used and if one of the 0900 h or 1500 h wind observations was missing, then the remaining value was used in the regression. The percentage variance accounted for

(adjusted for the degrees of freedom) for all the cases is low and similar low values were obtained when the wind stress rather than wind velocity was used. For the shallow water at the mooring sites in the Gulf, a higher correlation with the wind was expected. A possible explanation for the low correlations is that the winds at Mornington Island are not representative of the winds at the mooring sites due in part to sea breezes which occur diurnally at Mornington but would not be present well offshore at the mooring sites. Another reason for the low correlation may be that the wind distribution combines with the bathymetry and coastline to generate topographic gyres as found in the Great Lakes and elsewhere. The negative regression coefficients (not given) do indicate the current may flow counter to the wind events. During periods when tropical lows or cyclones were affecting the Gulf (Fig. 3) wind forced residuals of up to 0.25 m s^{-1} were recorded.

Two-dimensional Tidal Model

Diurnal Constituents

The co-tidal and co-range lines evaluated from the results of the model for the principal diurnal constituents K_1 and O_1 are shown in Figs 4 and 5. The agreement between the observed tidal constants and the computed results for the vertical tide and the tidal velocities is indicated in Table 3 and Table 4 respectively. For the vertical tide, the root mean square (rms) deviation between the model results and the observations is 0.08 m in amplitude, 16^{o} in phase for the K_1 tide and 0.06 m in amplitude, 13^{o} in phase for the O_1 tide.

For both constituents, the amplitude fit at Merauke, Edward River and Karumba is poorest and the phase fit is worst at the Northern Territory/Queensland border and Centre Island (see Table 3). Attempts were made to improve the amplitude fit at the above locations by adjusting the open boundary conditions but these resulted in an increase in rms

deviation over the rest of the model. Similarly, small improvements to the phase fit along the south-west coast were at the expense of the fit over the rest of the Gulf. While small discrepancies still exist, the overall agreement for the vertical tide is good and the results are generally similar to the results of Williams (1972) Reinecker (1979) and Webb (1981). It is possible that some of these discrepancies may be due to local phenomena (below the resolution of the model) in the vicinity of the tide gauge and poor estimation (from the field data) of the K_1 constants due to the neighbouring P_1 constituent.

For the northerly component of the tidal velocity, the results (with the exception of the phase of those off Arnhem Land) are in excellent agreement with observations. The poorer agreement for the easterly component may be due to lack of resolution of coastal features in the model and the inherent errors in estimating the easterly tidal component in the presence of a strong north-south signal. The poor results at Arnhem Land are thought to be a result of insufficient data (5 days) for evaluating the tidal components rather than a reflection of model inaccuracy.

The response of the Gulf for both constituents is very similar. There is one amphidrome (a region of small amplitude) near the centre of the Gulf (Figs 4 and 5) and the tide rotates around this point in a clockwise fashion. Comparison of the vertical tide and the tidal velocities at Weipa and Gove indicates that there is a travelling wave progressing around the Gulf.

Semi-diurnal Constituents

The co-tidal and co-range lines evaluated from the results of the model for the principal semi-diurnal constituents M_2 and S_2 are shown in Figs 6 and 7 and the agreement between the observed tidal constants and the computed results for the vertical tide and the tidal velocities are indicated in Tables 3 and 4 respectively. The response of the Gulf is

far more complex for the semi-diurnal constituents than for the diurnal constituents and the agreement between the model results and the measurements is not as good as for the diurnal constituents. The worst results are for the smallest constituent S_2 but even here there is still a qualitative agreement between the model results and the measurements. For the vertical tide, the rms deviation between the model results and the observations is 0.11 m in amplitude, 32^{o} in phase for the M_2 tide and 0.08 m in amplitude, 31^{o} in phase for the S_2 tide. Merauke, the Northern Territory/Queensland border and Centre Island locations have the poorest amplitude agreement for both constituents and the coast from Weipa to Karumba shows the poorest phase agreement. As with the diurnal constituents, adjustments to further improve the fit at these locations produced unacceptable increases in the rms deviation over the rest of the Gulf. In the south-eastern corner of the Gulf where the three current meter moorings were located, the amplitude of the semi-diurnal tidal velocities is typically less the 0.05 m s^{-1} for both north and east components. Despite this small magnitude, the model fits the observations well, particularly at the mooring location west of Mornington Island.

For the M_2 constituent, Easton (1970) indicated an amphidromic point at ~ 10^{o}S, 141^{o}E but suggested that further amphidromic points may occur near Mornington Island and Groote Eylandt. In Williams' (1972) analytical model in which rotation and dissipation were ignored, a standing wave with a nodal line running from the south-east corner of the Gulf to West Irian was excited. When rotation was included in the model, amphidromic points appeared on this line. Williams (1972) suggested that the inclusion of friction would alter the position of these amphidromes such that there would be an amphidrome near Mornington Island and Groote Eylandt and an amphidrome approximately midway between Cape York and Gove Peninsula. However, there were no model results to support this suggestion. The present results confirm the suggestions of

Easton (1970) and Williams (1972) concerning amphidromes near Mornington Island and Groote Eylandt. Between Cape York and Gove Peninsula, there is a region of low amplitude and rapid phase variations (as in the non-rotational model of Williams (1972)) but there is no amphidrome. At the False Cape end of Williams' nodal line, there is now a 0.9 m amplitude tide. Webb (1981) does not find an amphidrome near Groote Eylandt. Tidal measurements in the south west corner of the Gulf may help resolve this point.

Observations of Large Scale Residual Currents and Seasonal Variations in Mean Sea Level

Prior to the present study, the only direct observations of residual currents in the Gulf of Carpentaria were those of Cresswell (1971), which suggested a northward flow at Weipa for 4 nautical miles/day in winter and a southward flow of 1 nautical mile/day in summer. Newell (1973) discussed these observations in relation to currents inferred from hydrological observations.

From September 1978 until March 1979, 300 Woodhead sea bed drifters were released at widely distributed locations in the south-east Gulf and 12 window-blind buoys, drogued at 10 m, were deployed in October/November 1978 55.6 km apart along a line of latitude $16^{o}15'S$. Only 13 of the drifters were recovered and 5 sightings were made of the drogued buoys. The tracks of both are plotted in Fig. 8. Ten of the seabed drifters were recovered ashore several months after release, and showed no preferred drift direction. The low return of drifters is partly because of the low human population density along the coast although a higher number of returns was expected from the large trawling fleet. The majority of those window-blind buoys which were sighted subsequent to deployment drifted south-east, parallel to the north-west monsoons (dominant at this time of the year), and 3 were found ashore.

The first satellite-tracked buoy (No. 1104) was released in the centre of the Gulf in 1978. It made a clockwise circuit of the Gulf in 191 days at an average speed of 11.8 cm/s (Fig. 9). It was re-released in 1979 at a position 96 nautical miles north-west of centre and it again drifted clockwise around the Gulf, in 254 days at an average speed of 5.6 cm/s. Another buoy (No. 1202), released on day 232, 1980, remained almost stationary for 30 days before slowly moving off to the south-east at an average speed of 3.7 cm/s over 156 days. The last buoy (No. 1364) released on day 355, 1980, drifted parallel to No. 1202 for 52 days at an average speed of 7.4 cm/s.

Annual ranges of monthly mean sea levels were estimated from the data of Easton (1970) and unpublished data (G.W. Lennon, pers. comm.). The largest range (75 cm) is found at Karumba in the south-east corner, and ranges of 62 and 61 cm are found at Centre Island and Weipa respectively. Even at the extremities, Melville Bay and Red Island Point, the range is still large (44 and 39 cm respectively), compared with 24 cm at Darwin (outside the Gulf). A plot of monthly mean sea level for Darwin, Milner Bay and Centre Island (Fig. 10) shows that at all stations the annual variations are in phase, with peak levels occurring in January and minimum levels in July. The significance of this seasonal variation will become more apparent when we consider the annual variation of wind, atmospheric pressure and river run-off.

Models of Residual Currents

For calculating residual currents the model was run for a 15 day period (covering a spring-neap cycle) and the output (at hourly intervals) filtered with a low pass filter (Munk's "tide-killer" filter). For these runs, the four major tidal constituents (O_1, K_1, M_2, S_2) are combined as the forcing function at the open boundary and the tidal flow through Torres Strait is also specified.

In addition to modelling the tide-induced residual circulation, wind stress, as computed from wind velocities was also applied. Analysis of monthly wind frequency data for 10 Bureau of Meteorology stations around the Gulf (Fig. 1), shows that there is a smooth annual variation in amplitude between south-east trades (which peak in July) and north-west monsoons (which peak in January). Monthly mean wind stress at Weipa, which illustrates this variation, is given in Table 5.

A mean wind stress for each month at each station was calculated from these data and a smoothed grid of wind stress for the whole Gulf produced wind speeds for any given month are larger in the north than in the south, and this is reflected in the stress distribution. During July, the north-westward stress in the northern half of the Gulf ranges from 0.10 N m^{-2} in the west to 0.15 N m^{-2} in the east, while in the south, it is more uniform at 0.05 N m^{-2}. During January, the south-eastward stress in the northern half ranges from 0.08 N m^{-2} in the west to 0.06 N m^{-2} in the east, while in the south it is greatly reduced, to about 0.01 N m^{-2}.

If the wind observations at stations on the mainland were given equal weight with those on the islands, this spatial variation would be more pronounced, but the island winds are probably more representative of the wind in the interior of the Gulf than the mainland stations and were weighted accordingly to give a smoother distribution. At each grid point, the wind stress was the vector sum of the stress at all 10 stations, each weighted as the inverse square of its distance from any island station and as the inverse fourth power of its distance from any mainland station.

Tide Induced Residual Currents

Non-linear interactions of the first order tidal currents produce residual currents whose magnitude should vary in phase with the spring-neap cycle. The spring-neap cycle has a period of 13.66 days in the southern half of the Gulf where the diurnal constituents are dominant and a period of 14.76 days in the northern half of the Gulf where the semi-diurnal constituents are dominant. Residual tidal currents produced by the model for a period of spring tides are shown in Fig. 11. The modelled residual circulation is clockwise at about 3 cm/s for springs (although some currents are as strong as 8 cm/s) and 1 cm/s for neaps, which compares well with observation of satellite-tracked drogued buoys.

Wind Induced Currents

The model was run for the January wind stress distribution for spring and neap tides. The effect of this north west monsoon wind stress is to enhance the weak clockwise residuals of the tidal model (Fig. 12). For both spring and neap tides, the currents (with wind) are typically 4 cm/s in the north, 7 cm/s at the east perimeter and 10 cm/s on the western side. Residuals in the south east corner are approximately 1 cm/s. The north-east winds cause a rise in mean sea level at Karumba of 4 cm.

In addition to the wind stress distribution derived from monthly mean winds around the Gulf, a uniform NW wind stress of 0.140 N m^{-2} (8.5 m/s wind speed) was imposed on the tidal model, and the residual currents calculated (results not shown). This may represent the Gulf circulation in strong wind periods better than the mean stress distribution, which was based on land wind observations. The most significant difference with the increased wind stress is a southward flow past Groote Eylandt, and the creation of a anticlockwise gyre off Centre Island, together with a

strong NW flow, up to 6 cm/s at neaps and 3 cm/s at springs from the south-east corner.

Under the influence of the south-east trades, the model's weak clockwise neap tide residual currents (generally less than 1 cm/s) are reversed in the northern half of the Gulf (Fig. 13) creating an anti-clockwise gyre centred on 12^{o}S, 140^{o}E. A strong northerly flow along the eastern side of the Gulf, up to 15 cm/s, characterizes this circulation. In the southern portion of the Gulf below 15^{o}S there is a slow clockwise circulation typically 3 cm/s, centred 55 km north east of Centre Island.

During springs, both tidal and residual currents are stronger. Thus bottom stresses are larger, so the trade wind driven flow is reduced, and this flow makes a smaller contribution to the total residual. The clockwise tidal residual currents are reduced to about 2 cm/s and a smaller, anticlockwise gyre, with maximum currents of 8 cm/s is generated in the north-east (see Fig. 14), centred off Port Musgrave. The south-east winds cause a fall in mean sea level of 18 cm at Karumba.

A uniform wind stress of 0.140 N m^{-2} (wind speed of 8.5 m/s) from the south-east was also applied to the model to investigate the response of the Gulf to larger wind stress. The only significant difference was in the south-east corner of the Gulf where onshore currents of 6 cm/s at neaps and 2 cm/s at springs were generated.

Steric Height Variations and Density Currents

In this section variations in mean sea level due to variations in density of the water column (steric sea level changes) are discussed. Density changes arise as a result of heat gain or loss through the surface, evaporation, and fresh water input (from direct precipitation and river run-off).

The steric height anomaly at Karumba calculated from data collected during 7 cruises in 1976-78 was plotted, and although the seven cruises are not well spaced in time, there appears to be an annual cycle, with a September minimum of -6.2 cm and an April maximum of 12.6 cm. This variation appears to lag behind the average monthly variations of mean sea level by about 2 months.

Vertical current shears will be set up to balance horizontal density variations. During the monsoon season, river run-off results in less dense water occurring around the perimeter of the Gulf. The resulting density gradients will induce a surface clockwise geostrophic circulation relative to the bottom circulation. For the situation in May 1976 assuming zero bottom current, the resulting westward flow 25 km offshore of Karumba would be 6.8 cm/s. During the trade wind season, the centre of the Gulf may become less dense than the perimeter (due to nearshore evaporation and heat loss) and a small anticlockwise circulation of 1 cm/s may develop.

Because of the shallowness of the Gulf and the strong tidal currents, it is expected that the above geostrophic currents will be affected by friction. Heaps (1972) obtained an Ekman-like solution which involves a balance between the Coriolis force, the pressure gradient and frictional shear stress. The solution for well mixed conditions with σ_t lines parallel to the coast gives onshore flow near the bottom and a clockwise rotation of the velocity vectors (in the southern hemisphere) with increasing height above the seabed. This method was applied to the situation in March 1977 to determine the shoreward and longshore components of the density currents for the east side of the Gulf where the strongest horizontal density gradients existed. The maximum currents are produced 74 km offshore where an onshore bottom current of 2.3 cm/s (071^{o} true), a longshore current of 1.4 cm/s and an offshore surface current of 3.4 cm/s (267^{o} true) are predicted (Fig. 15). As the shore is approached the magnitudes of these currents decrease.

When the geostrophic currents due to surface slope were calculated earlier, they were by definition, perpendicular to the section and directed alongshore. In comparison to the model of Heaps, the geostrophic calculation appears to overestimate the currents by a factor of two because it neglects friction.

Hydrostatic Level

Another factor which contributes to mean sea level variation is the hydrostatic response of the Gulf to changes in atmospheric pressure. Pressure at a number of Bureau of Meteorology stations was compared around the Gulf, and each monthly mean was found to be nearly uniform over the Gulf. There is an annual cycle of atmospheric pressure variation, with a maximum in July (minimum sea level) and a minimum in January (maximum sea level). Assuming that a 1 mbar change in pressure yields a 1 cm change in sea level, mean sea level at Karumba rises by 5.3 cm in January and falls by 4.2 cm in July.

Vertical Current Structure and Advection of Larvae

The three-dimensional model was used to generate hourly current profiles. The current meter observations reported earlier were used to adjust the parameter in the model so that measurements and the model results were in close agreement. In both the measurements and the model the ratio of the velocities at heights in the water column corresponding to the location of the current meters was approximately 0.85. Also, there was little change in direction of the current with depth at time of maximum velocity and near the change of tide there was a greater change in direction with depth (up to 40^{o}). The two- and three-dimensional models were also in close agreement with the depth averaged velocity lying between the surface and bottom velocities of the three-dimensional model. The months when the three-dimensional

model was applied (March and October) was the changeover in seasons and winds were light. The small changes that occurred in the surface velocity of the three-dimensional model were as expected in the direction towards which the wind was blowing.

The simplest scheme to test the effect of the currents on the movement of larvae was to use the depth averaged velocities and to assume a) the larvae do not migrate vertically and b) the larvae move into the water column during the night but during the day they either settle on the bottom or at least remain very close to the bottom.

The two main locations for the release of larvae were considered. These locations correspond to the centre of spawning grounds 100 km north-north-east of Karumba and 50 km west of Weipa. The larvae were advected with the ambient current for 20 days by which they must reach the estuarine nursery grounds or perish. When there was no vertical migration there was very little net movement of the larvae over the 20 days. Near Karumba there was a movement of 10 km west in both seasons and near Weipa there was a movement of 50 km north in October and 30 km south in March.

When vertical migration was introduced this picture changed dramatically. In March, the Weipa larvae moved north-east ~ 100 km and at Karumba they moved north-west ~ 100 km. In October, this picture was reversed and the larvae near Weipa moved south ~ 100 km and the larvae near Karumba moved south-south-east ~ 100 km almost directly towards the mouth of the Norman River.

The results of using the three-dimensional model currents and various more sophisticated vertical migration schemes change the quantitative figures but the general picture remains the same; i.e. little movement when no vertical advection is considered and movement to the north at both sites in March and to the south in October when vertical migration was included. The last

day for which spawning can occur in the southern region and the larvae reach the Norman River is approximately 25 November (the exact date will be affected by the vertical migration scheme chosen). After this date the larvae are carried north away from the Norman River.

Discussion

The direct current meter observations support the historical data which suggested that the tidal currents are an order of magnitude larger than the residual currents. Although the near bottom currents are not quite as strong as the mid-depth currents, there is little variation in direction or phase of the tidal currents with depth. These observations combined with the fact that the Gulf is well-mixed for much of the year means that a two-dimensional model should be suitable for simulating tidal and wind driven currents. This belief was confirmed by the excellent agreement between the observed and computed tidal heights and tidal currents.

The agreement between the measured and modelled residual currents and mean sea level was also good.

The satellite-tracked buoy data indicate a clockwise circulation of 3.7 to 11.8 cm/s. This is in good agreement with the modelled tidal residuals, north-west monsoon-driven currents and density induced currents at mid-depth which range from 1 to 10 cm/s.

Direct evidence for the location of the centre of the clockwise gyre comes from a satellite-tracked buoy which was launches at 12.4^{o}S, 139^{o}E in 1980. It moved 20 km then remained within 10 km of this position for 30 days, suggesting that it was in a region of very small currents near the centre of a gyre.

The only model results that do not show clockwise circulation are those for south-east trade winds. There is evidence from two of the satellite-tracked buoys that during the trade wind season, a north-

westward residual current of 5-8 cm/s exists in the southern part of the Gulf. However, with trade wind stress, only during spring tides does the model show north-westward currents of 2 cm/s. The balance between wind driven and tide induced residuals is obviously critical, since they are of the same order, so in months of smaller trade wind stress, and during spring tides, the general Gulf circulation is more likely to be clockwise than anticlockwise.

A shoreward bottom current in the south-eastern corner of the Gulf is indicated by the fact that ten of the thirteen bottom drifters recovered were found ashore. The numerical model of density induced currents also indicates a shoreward component at the bottom. However, as the shore is approached these currents decrease, so in very shallow water, wave transport and tidal residuals may become more important.

The observed range in monthly mean sea level for Karumba is 75 cm. Wind stress, atmospheric pressure and density effects contribute 22.5, 19 and 9.5 cm respectively, the sum of which is 51 cm, approximately two thirds of the observed range. The reason for the unaccounted variance may lie in underestimation of wind stress in either of the two seasons and in variations in mean sea level in the Arafura Sea, both of which are outside the scope of the present work.

The results of combining the computed currents with the vertical movement of larvae was extremely successful. For the Weipa area, the March larvae are carried north-north-east while the October larvae are carried south. This is consistent with Staples (1979) who found that in the area north of Weipa the March spawning was the most successful.

In the Karumba area, it is the October spawning that goes to make the March fishing stock and the March spawning is unsuccessful. This is because the October larvae are carried toward the estuaries whereas the March larvae are carried away from the estuaries and lost to the fishery.

The last day that larvae spawned offshore from Karumba can be carried shoreward is approximately 25 November. This corresponds very closely with the data of 1 December after which Staples (personel communication) finds no more larvae entering the Norman River.

The reason for this differential advection is that from October to March the phase of the diurnal tide varies by 180^{o} and this change in phase combines with the diurnal vertical migration of the larvae to change the direction of movement of the larvae.

This project has answered many of the questions about the circulation in the Gulf of Carpentaria and has also identified specific questions for further work. These relate to the tidal characteristics in the centre of the Gulf, in the area north of Gove and in the south-west corner of the Gulf. Of particular concern in the present study was the lack of good meteorological and current data in the centre of the Gulf. Although it appears that the flow through Torres Strait is not of major importance for Gulf circulation, there needs to be more work to clarify this point.

This cooperative study between physical oceanographers and fisheries biologists has been very successful in showing how a combination of physical and biological factors affect larval disperson distances and direction. Though it has answered many questions there are still some important areas left to be investigated. The following are two of the most important biological questions. Firstly, in order to understand the importance of larval mortality in determining the year to year variation in abundance of adult stocks we need to look at environmental factors affecting larval dispersal during critical times of the year over a number of years. Secondly, along with more detailed studies of adult and juvenile habitat requirements, of a number of commercially important penaeid species, we will need detailed assessment of local current regimes which establish the larval-dispersal-link between these discrete species specific adult and juvenile habitats.

References

Buchwald, V.T., and Williams, N.V. (1975). Rectangular resonators on infinite and semi-infinite channels. *Journal of Fluid Mechanics* 67, 497-511.

Cresswell, G.R. (1971). Current measurements in the Gulf of Carpentaria. Australia CSIRO Division of Fisheries and Oceanography Report No. 50.

Easton, A.K. (1970). The tides of the continent of Australia. Horace Lamb Center for Oceanographic Research, Research Paper No. 37.

Easton, A.K. (1977). Selected programs for tidal analysis and prediction. Flinders Institute for Atmospheric and Marine Sciences. Computing Report No. 9.

Garcia, S., and Le Reste, L. (1981). Cycles vitaux, dynamique, exploitation et aménagement des stocks de crevettes penaéïdes côitères. FAO Tech. Doc. Fisheries No. 203, 210 p.

Heaps, N.S. (1972). Estimation of density currents in the Liverpool Bay area of the Irish Sea. *Geophysical Journal of the Royal Astronomical Society* 30, 415-32.

Jelesnianski, C.P. (1970). Bottom stress time history in linearized equations of motion for storm surges. *Monthly Weather Review* 98, 462-78.

Jordon, T.F., and Baker, J.R. (1980). Vertical structure of time dependent flow dominated by friction in a well-mixed fluid. *Journal of Physical Oceanography* 10, 1091-1103.

Melville, W.K., and Buchwald, V.T. (1976). Oscillations in the Gulf of Carpentaria. *Journal of Physical Oceanography* 6, 394-8.

Newell, B.S. (1973). Hydrology of the Gulf of Carpentaria. Australia CSIRO Division of Fisheries and Oceanography Technical Paper No. 35.

Penn, J.W. (1975). The influence of tidal cycles on the distributional pathway of *Penaeus latisulcatus* Kishinouye in Shark Bay, Western Australia. *Australian Journal of Marine and Freshwater Research* 26, 93-102.

Reinecker, M.M. (1979). Tidal propagation in the Gulf of Carpentaria. Ph.D. Thesis, University of Adelaide.

Rochford, D.J. (1966). Some hydrological features of the eastern Arafura Sea and he Gulf of Carpentaria in August 1964. *Australian Journal of Marine and Freshwater Research* 17, 31-60.

Rothlisberg, P.C. ( ). Vertical migration and its effect on dispersal of penaeid shrimp larvae in the Gulf of Carpentaria, Australia. *Fisheries Bulletin, U.S.* (in press).

Staples, D.J. (1979). Seasonal migration patterns of postlarval and juvenile banana prawns, *Penaeus merguiensis* de Man, in the major rivers of the Gulf of Carpentaria, Australia. *Australian Journal of Marine and Freshwater Research* 30, 143-57.

Staples, D.J. (1980). Ecology of juvenile and adolescent banana prawns, *Penaeus merguiensis*, in a mangrove estuary and adjacent offshore area of the Gulf of Carpentaria. I. Immigration and settlement of postlarvae. *Australian Journal of Marine and Freshwater Research* 31, 635-52.

Webb, D. (1981). A numerical model of the tides in the Gulf of Carpentaria and the Arafura Sea. *Australian Journal of Marine and Freshwater Research* 32, 31-44.

Williams, N.V. (1972). The application of resonators and other methods to problems in oceanography. Ph.D. Thesis, University of New South Wales.

Table 1. Current meter locations and statistics of records

	Position	Station code	Water depth (m)	Meter depth (m)	Length of series (h)	Average variance about mean ($cm^2\ s^{-2}$)	Average tidal variance ($cm^2\ s^{-2}$)	Residual tidal variance %	Mean northward component ($cm\ s^{-1}$)	Mean eastward component ($cm\ s^{-1}$)
Mooring 1	16°15.25'S 140°50.09'E	GC	20	9	2 842	655	646	4	0.1	-0.9
	16°15.25'S 140°50.09'E	GD	20	14	1 673	514	511	5	0.9	-1.3
Mooring 2	16°59.05'S 140°21.09'E	GE	17	6	1 527	779	765	5	1.7	-2.7
	16°59.05'S 140°21.09'E	GF	17	9	3 246	485	449	11	1.3	-1.0
Mooring 3	16°27.06'S 130°00.00'E	GG	18	7	2 204	211	181	13	0.4	0.1
	16°27.06'S 139°00.00'E	GH	18	12	2 209	169	146	10	1.0	-0.4

Table 2. The four major tidal constituents for the six records. The amplitudes H are in cm s^{-1} and the phases g in degrees. The phases are Greenwich phase lags for time zone -10 h (g(-10)).

(N.C. - Northward Component. E.C. - Eastward Component).

Location		O_1		K_1		M_2		S_2	
Code		N.C.	E.C.	N.C.	E.C.	N.C.	E.C.	N.C.	E.C.
GC	H	20 ± 1	2.7 ± 0.6	33 ± 2	3.5 ± 0.8	3.2 ± 0.3	2.0 ± 0.3	2.7 ± 0.3	1.0 ± 0.1
	g	343 ± 3	157 ± 13	33 ± 3	159 ± 13	261 ± 5	47 ± 9	80 ± 5	100 ± 9
GD	H	16 ± 1.6	1.6 ± 0.2	28 ± 2.8	3.0 ± 0.5	2.4 ± 0.6	1.5 ± 0.2	2.2 ± 0.5	1.0 ± 0.3
	g	348 ± 6	159 ± 9	61 ± 6	191 ± 9	278 ± 13	61 ± 16	104 ± 13	109 ± 16
GE	H	20 ± 1	4 ± 1	32 ± 2	7 ± 2	5.7 ± 0.6	1.4 ± 0.5	1.6 ± 0.2	1.4 ± 0.5
	g	355 ± 3	31 ± 17	60 ± 3	100 ± 17	258 ± 8	344 ± 19	90 ± 8	38 ± 19
GF	H	17 ± 1	2.6 ± 0.5	27 ± 2	6 ± 1	4.7 ± 0.7	2.4 ± 0.4	1.9 ± 0.3	1.1 ± 0.2
	g	349 ± 5	77 ± 10	62 ± 5	134 ± 10	273 ± 9	37 ± 9	85 ± 9	109 ± 9
GG	H	11 ± 17	6 ± 1	15 ± 2	7 ± 1	4.2 ± 0.6	6.6 ± 0.7	0.9 ± 0.1	2.1 ± 0.2
	g	325 ± 6	122 ± 9	52 ± 6	199 ± 9	145 ± 9	97 ± 6	175 ± 9	178 ± 6
GH	H	8 ± 1	4.7 ± 0.6	11 ± 1	8 ± 1	4.4 ± 0.4	6.3 ± 0.4	0.9 ± 0.1	1.9 ± 0.1
	g	329 ± 6	108 ± 8	44 ± 6	179 ± 8	145 ± 5	102 ± 4	194 ± 5	178 ± 4

Table 3. Comparison of observed and computed vertical tide for four constituents at nine locations (amplitudes in metres)

Constituent		K_1		O_1		M_2		S_2	
Location		Obs.	Comput.	Obs.	Comput.	Obs.	Comput.	Obs.	Comput.
Merauke	Amp.	0.68	0.82	0.55	0.61	1.26	1.14	0.46	0.30
	Phase	016	030	310	329	119	157	213	237
Booby Is.	Amp.	0.77	0.66	0.43	0.44	0.73	0.73	0.14	0.24
	Phase	048	044	352	350	203	213	312	288
Weipa	Amp.	0.46	0.41	0.31	0.30	0.36	0.34	0.10	0.14
	Phase	067	054	021	005	219	174	275	238
Edward R.	Amp.	0.47	0.57	0.39	0.48	0.07	0.16	0.05	0.11
	Phase	124	133	069	071	150	189	241	273
Karumba	Amp.	0.91	1.04	0.66	0.79	0.17	0.17	0.04	0.10
	Phase	181	173	118	108	250	310	026	079
N.T./Qld Border	Amp.	0.52	0.54	0.43	0.46	0.24	0.10	0.07	0.02
	Phase	203	170	118	103	089	093	187	204
Centre Is.	Amp.	0.40	0.42	0.35	0.38	0.34	0.12	0.11	0.03
	Phase	208	184	137	113	122	104	212	165
Groote Ey.	Amp.	0.17	0.16	0.17	0.15	0.29	0.30	0.12	0.14
	Phase	234	226	137	138	349	346	081	068
Gove	Amp.	0.28	0.28	0.20	0.18	0.74	0.62	0.25	0.24
	Phase	313	312	246	250	333	333	048	050

Table 4. Comparison of east and north components of observed and modelled horizontal tide for four constituents at five locations

(amplitudes in metres)

Location		K_1				O_1				M_2				S_2			
		East		North		East		North		East		North		East		North	
		Obs.	Modl.	Obs.	Modl.	Obs.	Modl.	Obs.	Modl.	Obs.	Modl.	Obs.	Modl.	Obs.	Modl.	Obs.	Modl.
No. 1 mooring	Amp.	0.03	0.08	0.32	0.32	0.03	0.06	0.20	0.23	0.02	0.03	0.03	0.06	0.01	0.02	0.02	0.04
Mid depth	Phase	045	069	265	255	018	008	204	189	117	143	331	033	160	233	140	130
No. 2 mooring	Amp.	0.07	0.04	0.32	0.32	0.04	0.03	0.19	0.23	0.01	0.02	0.05	0.07	0.01	0.01	0.02	0.03
Mid depth	Phase	310	310	270	267	252	241	216	202	054	124	328	050	098	227	150	172
No. 3 mooring	Amp.	0.06	0.05	0.14	0.11	0.06	0.03	0.10	0.09	0.06	0.03	0.04	0.02	0.02	0.01	0.01	0.01
Mid depth	Phase	049	038	262	257	343	333	186	192	167	171	215	175	238	231	234	235
Weipa	Amp.			0.23	0.20			0.15	0.15			0.17	0.07			0.04	0.01
(Cresswell)	Phase			253	254			207	187			093	100			149	167
Arnhem	Amp.			0.39	0.31			0.31	0.29			0.28	0.19			0.11	0.06
(Cresswell)	Phase			350	234			292	171			218	220			269	284

Table 5. Monthly mean windstress and direction towards which the wind blows at Weipa (1959-79)

Month	Jan.	Feb.	Mar.	Apr.	May	June	July	Aug.	Sept.	Oct.	Nov.	Dec.
Windstress (Nm^{-2})	.010	.008	.002	.011	.014	.014	.018	.012	.017	.012	.002	.001
Direction (degrees)	130	116	105	282	288	292	290	289	282	279	325	117

Figure Captions

Fig. 1. Location guide for the Gulf of Carpentaria.

Fig. 2. Major and minor ellipse axis for the K_1 consistuent at mooring 1(a), 2(b) and 3(c) and for the M_2 constituent at mooring 1(d), 2(e) and 3(f). The solid lines indicate the upper meter and the dotted lines the lower meter. All currents rotate clockwise unless indicated. Note the scale on a, b and c is different from d, e and f.

Fig. 3. Stick plots for the data after application of a low pass "tide-killer" filter. Times of cyclones (T.C.) and tropical lows (T.L.) are also indicated.

Fig. 4. Computed co-tidal lines (phase lag G) and co-amplitude lines (metres) for the K_1 constituent in the Gulf of Carpentaria.

Fig. 5 Computed co-tidal lines (phase lag G) and co-amplitude lines (metres) for the O_1 constituent in the Gulf of Carpentaria.

Fig. 6. Computed co-tidal lines (phase lag G) and co-amplitude lines (metres) for the M_2 constituent in the Gulf of Carpentaria.

Fig. 7. Computed co-tidal lines (phase lag G) and co-amplitude lines (metres) for the S_2 constituent in the Gulf of Carpentaria.

Fig. 8. Woodhead seabed drifter tracks (dahsed lines) and window-blind drogue tracks (solid line) in the south-east corner of the Gulf of Carpentaria. Day number and year of release and recovery are indicated. Also included are the locations of the three current meter moorings of 1978/79.

Fig. 9. Satellite-tracked drogued buoy tracks in the Gulf of Carpentaria. Selected day numbers and years are annotated. Buoy 1104 released day 359/1978. Buoy 1104 re-released day 293/1979. Buoy 1202 released day 232/1980. Buoy 1364 released day 355/1980.

Fig. 10. Monthly mean sea level for Centre Island, Milner Bay and Darwin from 1973 to 1977.

Fig. 11. Residual current vectors on a 15 n mile grid generated from the two-dimensional numerical model of Church and Forbes (1981). This frame shows Lagrangian currents at spring tides.

Fig. 12. Residual current vectors at spring tides for January monsoon wind stress.

Fig. 13. Residual current vectors at neap tides for July trade wind stress.

Fig. 14. Residual current vectors at spring tides for July trade wind stress.

Fig. 15. Plot of density current vectors at selected distances offshore, due to horizontal density gradient, after the method of Heaps (1972). At each location, vectors are plotted at fractional depths as indicated.

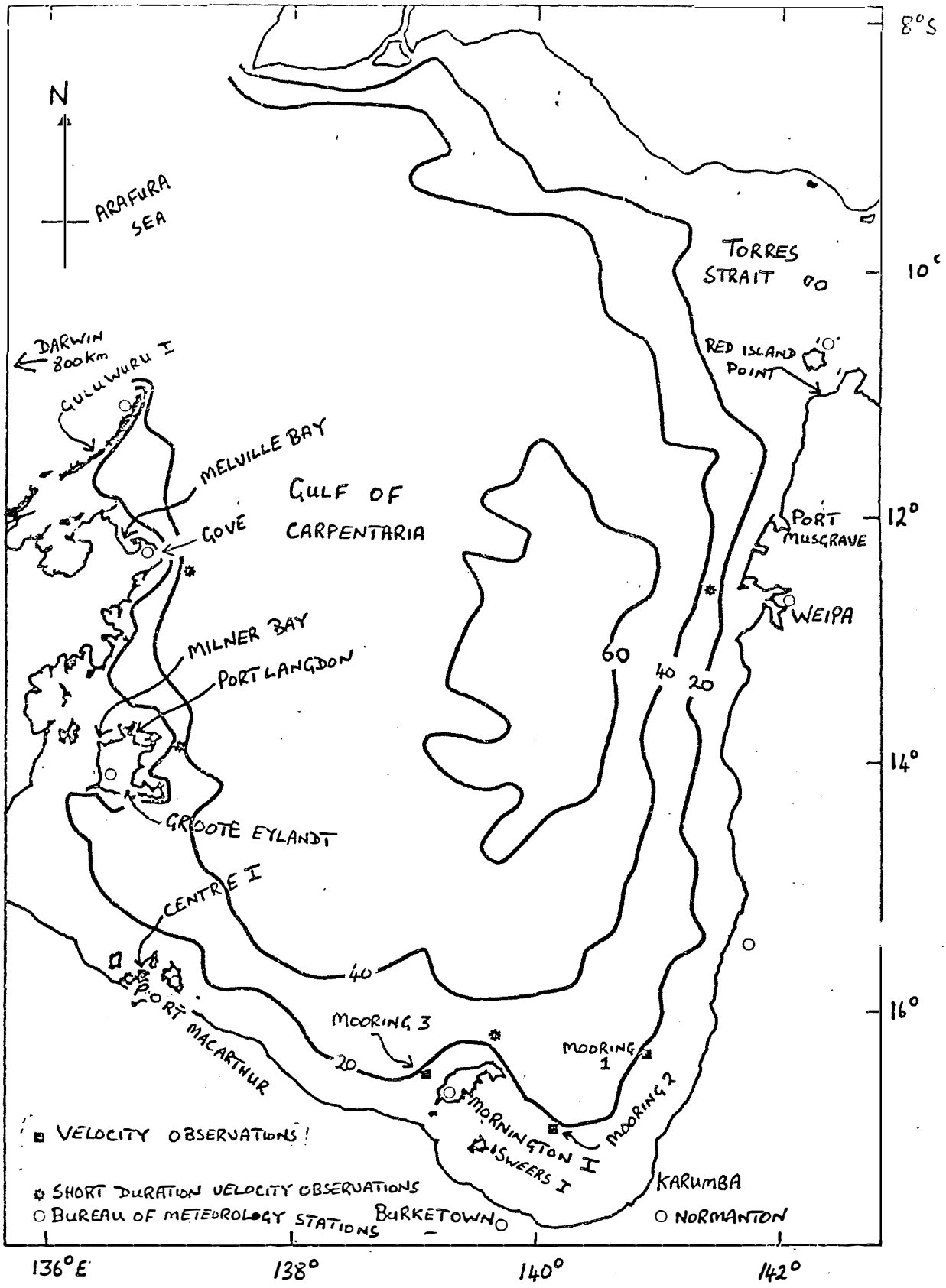

Fig. 1. Location guide for the Gulf of Carpentaria.

FIG 1

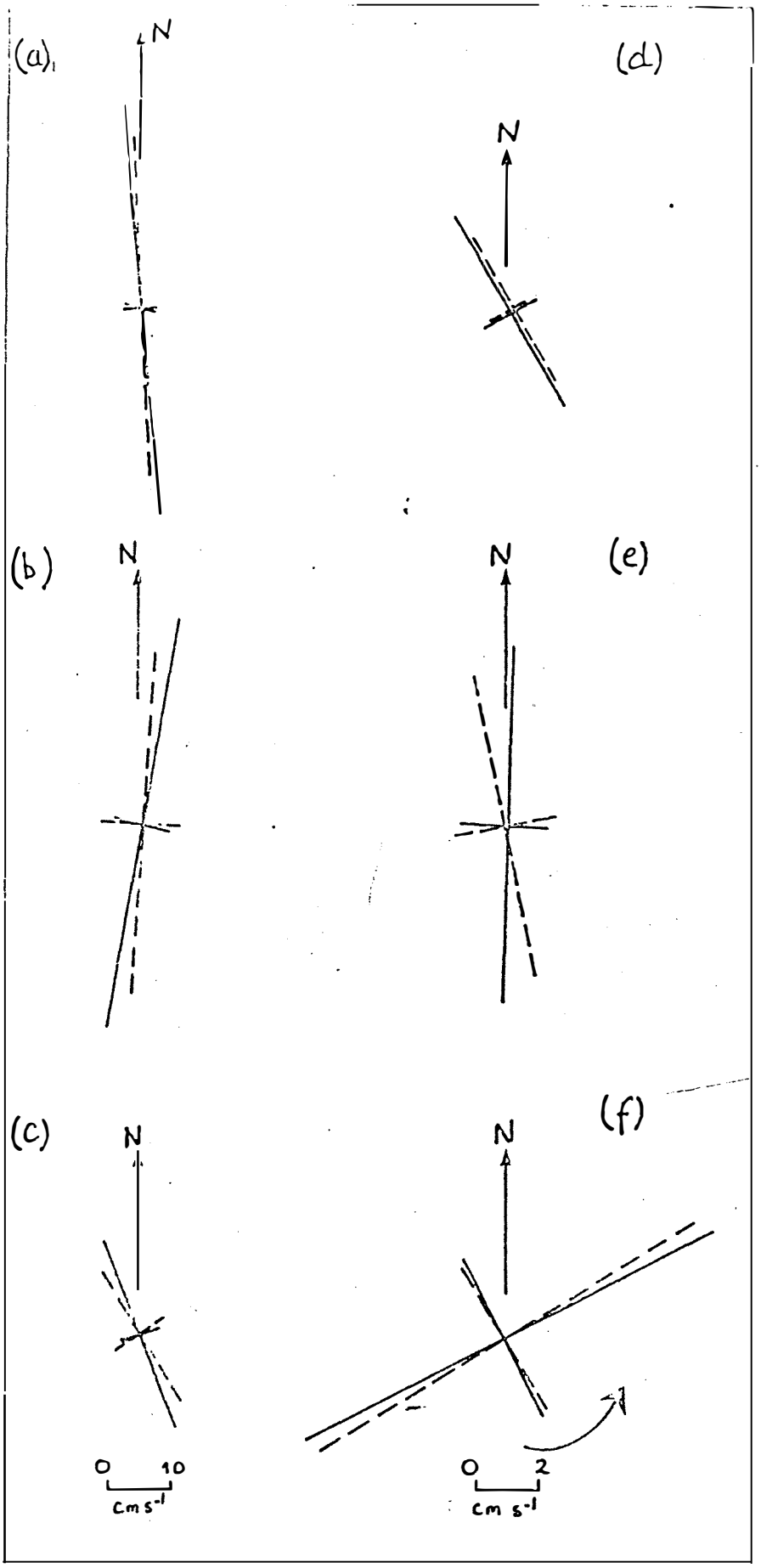

Fig. 2. Major and minor ellipse axis for the K_1 consistuent at mooring 1(*a*), 2(*b*) and 3(*c*) and for the M_2 constituent at mooring 1(*d*), 2(*e*) and 3(*f*). The solid lines indicate the upper meter and the dotted lines the lower meter. All currents rotate clockwise unless indicated. Note the scale on *a*, *b* and *c* is different from *d*, *e* and *f*.

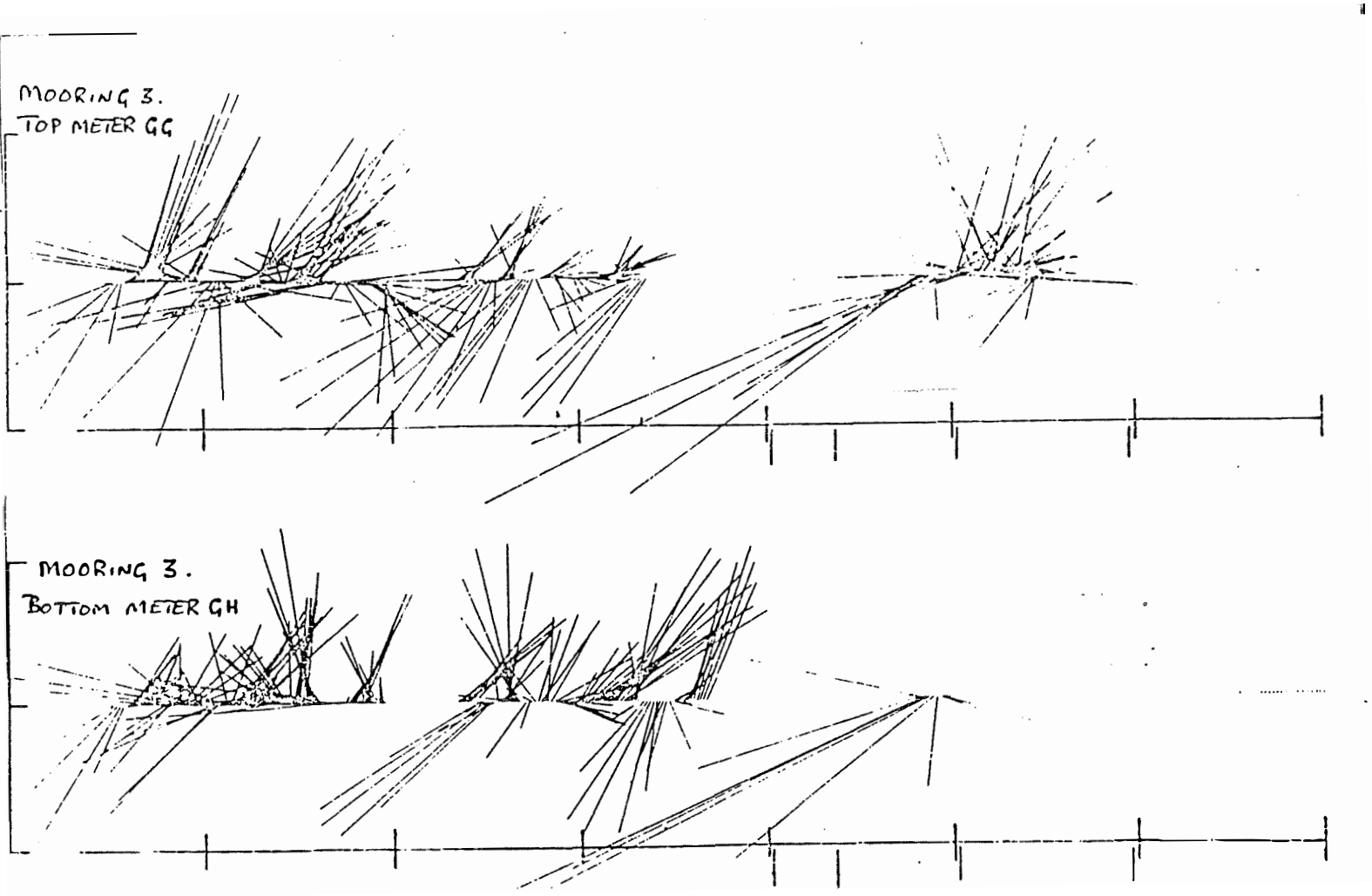

Fig. 3. Stick plots for the data after application of a low pass "tide-killer" filter. Times of cyclones (T.C.) and tropical lows (T.L.) are also indicated.

MOORING 1 . TOP METER GC

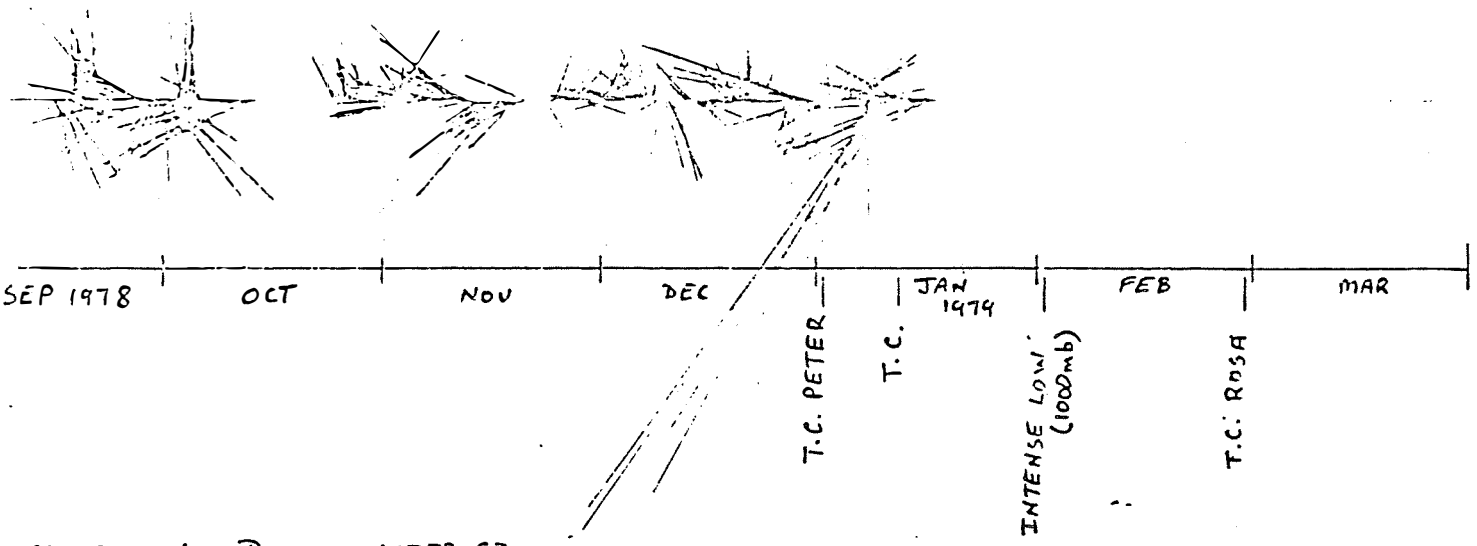

MOORING 1. BOTTOM METER GD

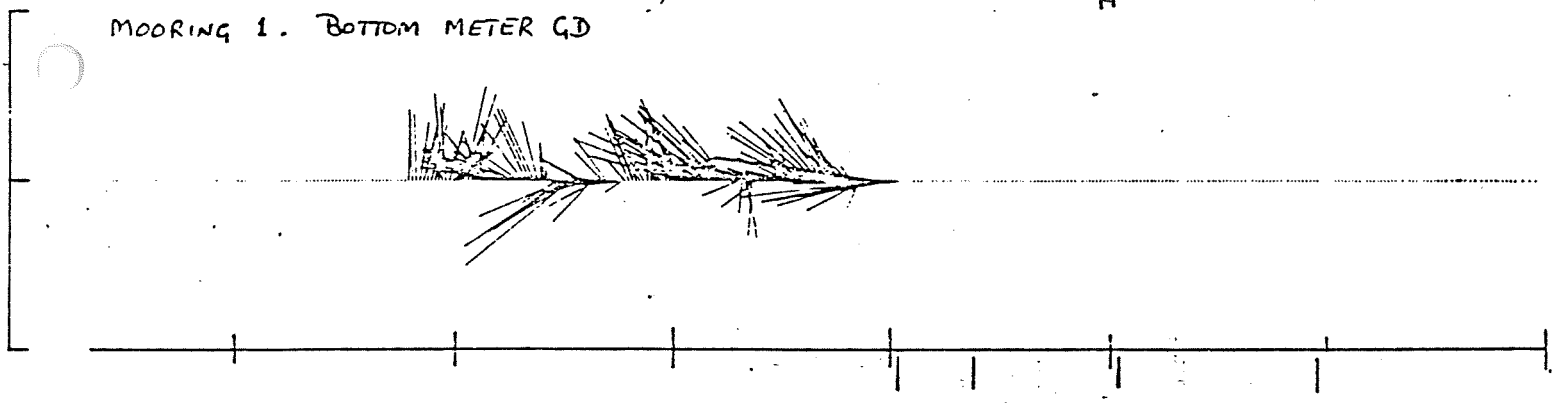

MOORING 2. TOP METER GE

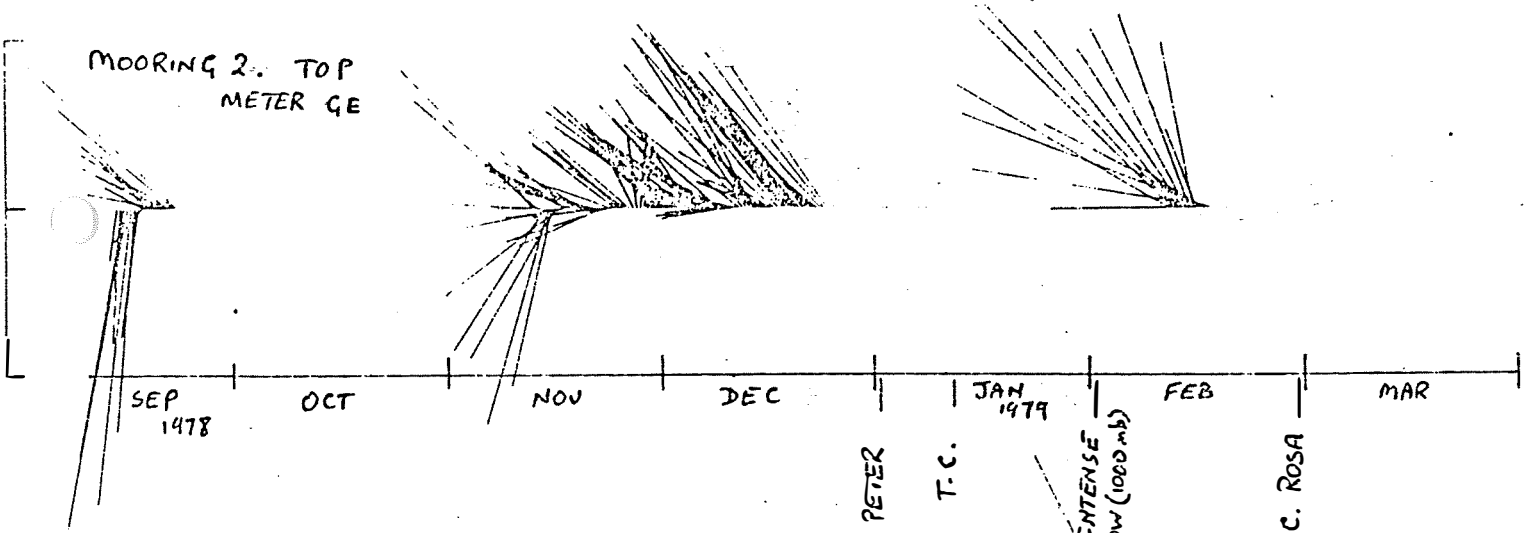

MOORING 2. BOTTOM METER GF

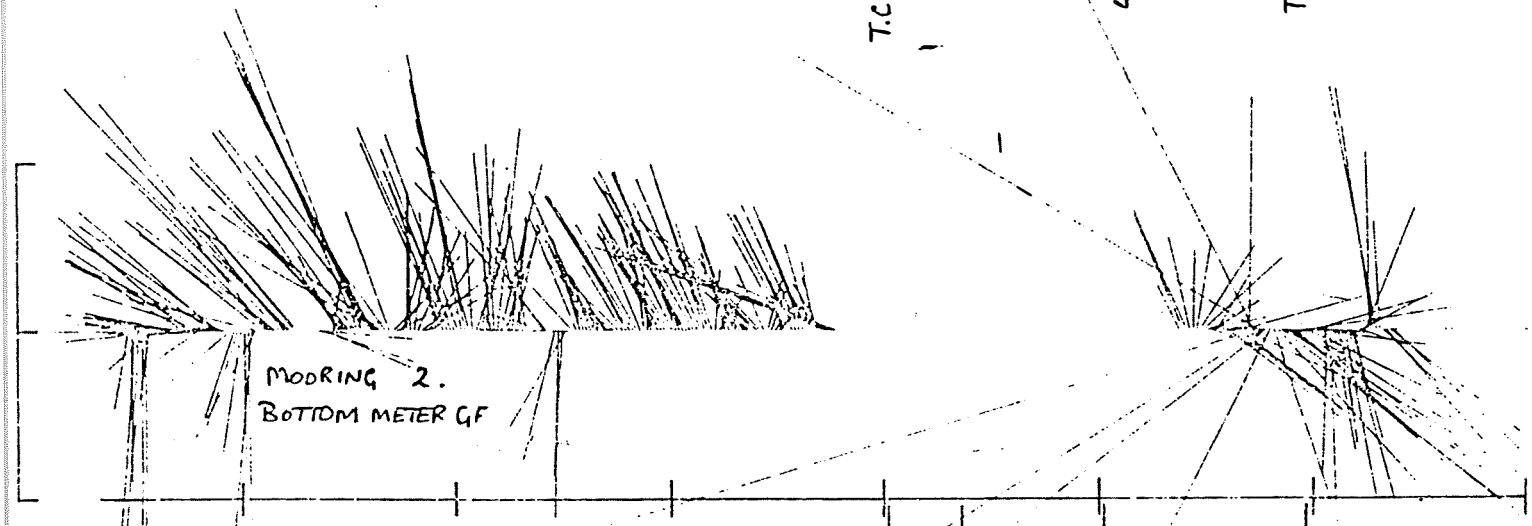

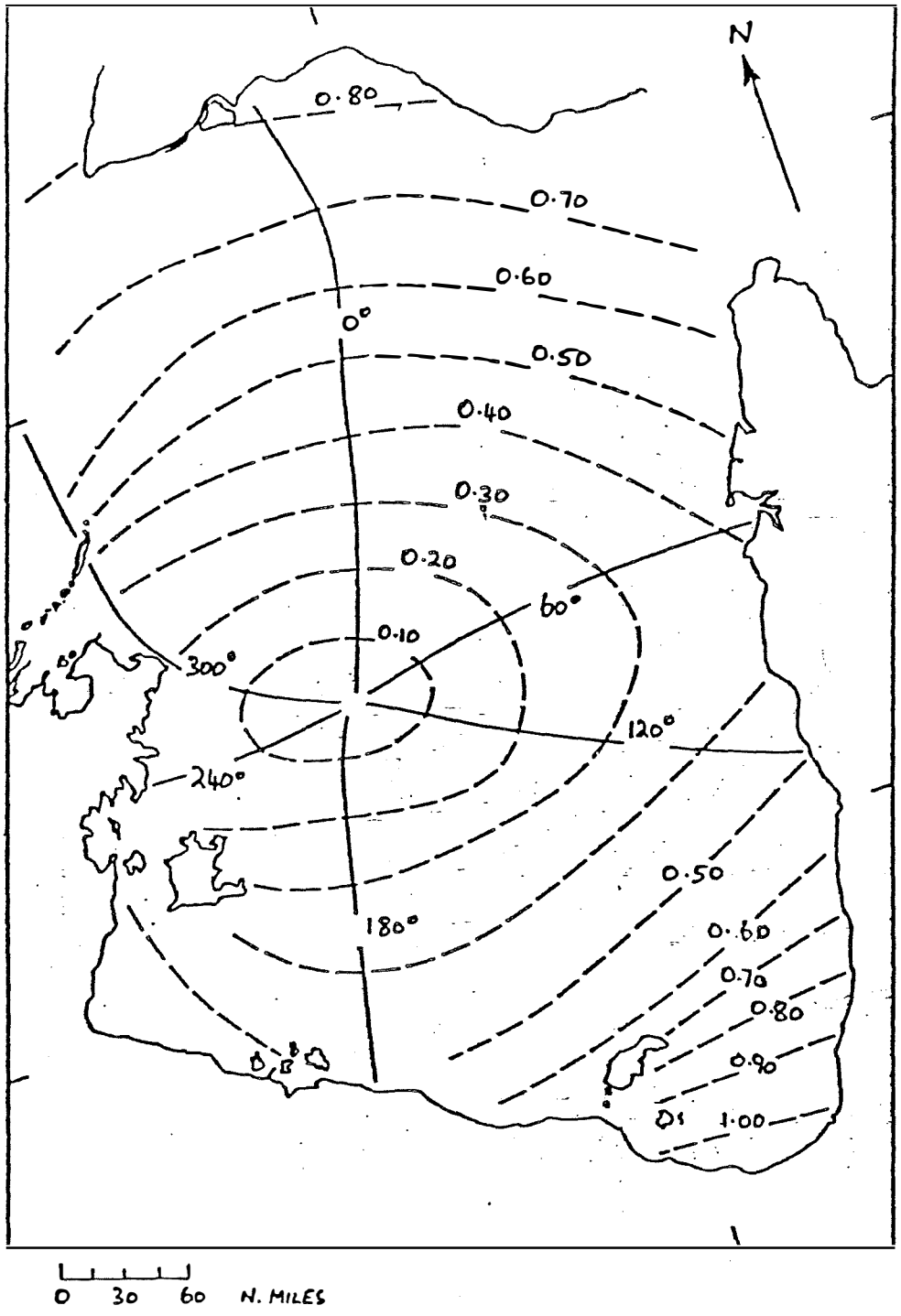

Fig. 4. Computed co-tidal lines (phase lag G) and co-amplitude lines (metres) for the K_1 constituent in the Gulf of Carpentaria.

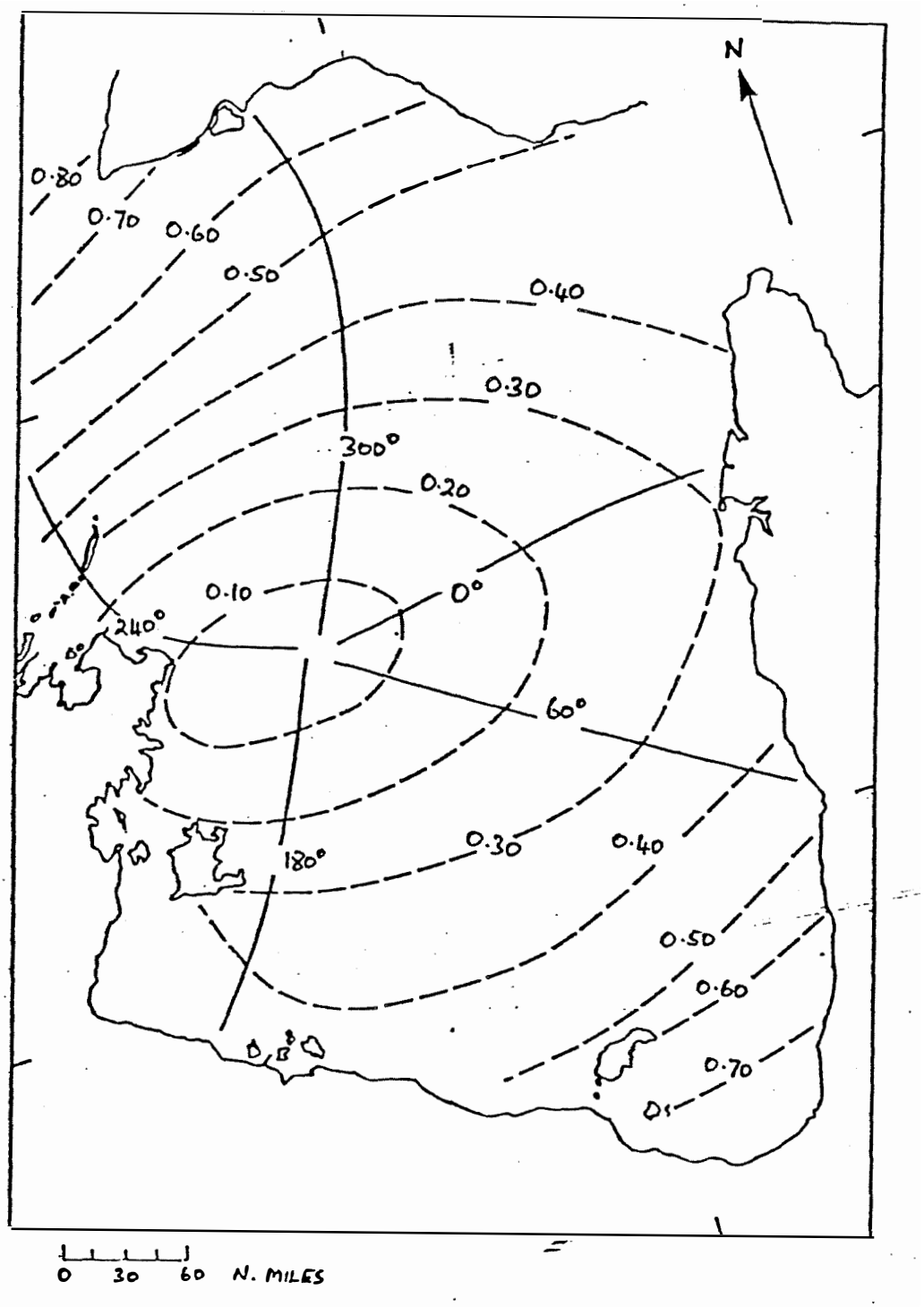

Fig. 5 Computed co-tidal lines (phase lag G) and co-amplitude lines (metres) for the O_1 constituent in the Gulf of Carpentaria.

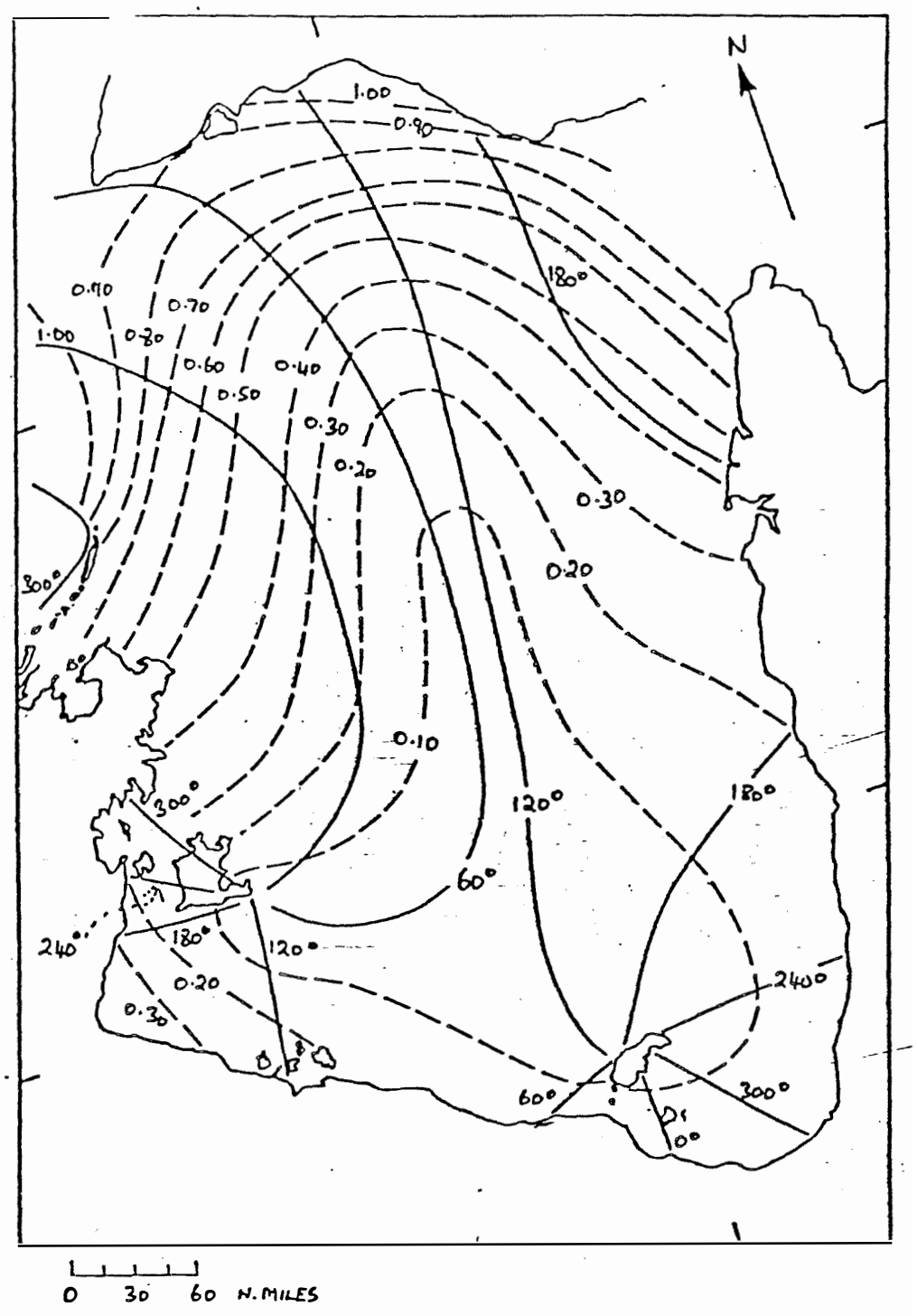

Fig. 6. Computed co-tidal lines (phase lag G) and co-amplitude lines (metres) for the M_2 constituent in the Gulf of Carpentaria.

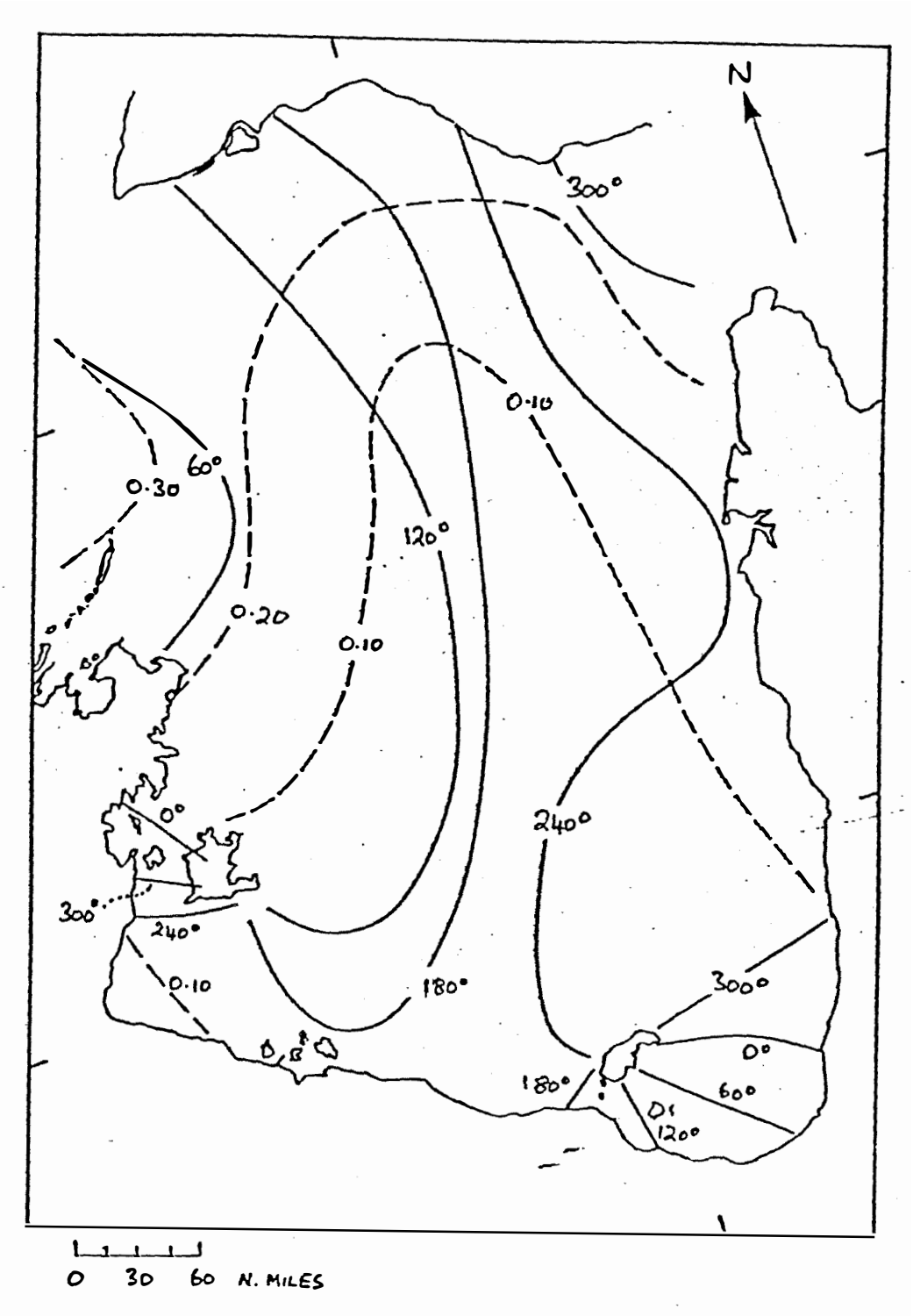

Fig. 7. Computed co-tidal lines (phase lag G) and co-amplitude lines (metres) for the S_2 constituent in the Gulf of Carpentaria.

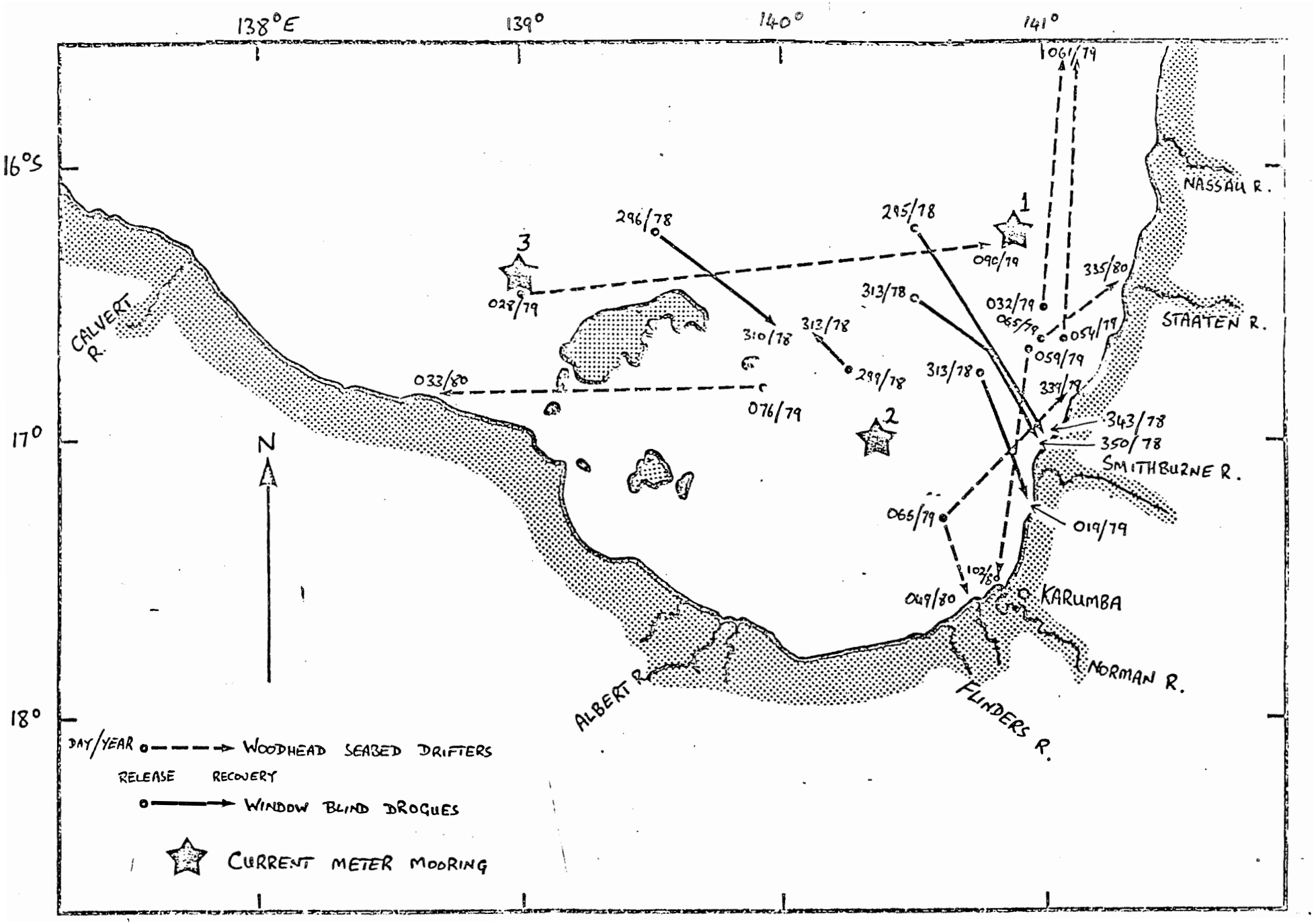

Fig. 8. Woodhead seabed drifter tracks (dahsed lines) and window-blind drogue tracks (solid line) in the south-east corner of the Gulf of Carpentaria. Day number and year of release and recovery are indicated. Also included are the locations of the three current meter m ings of 1978/79.

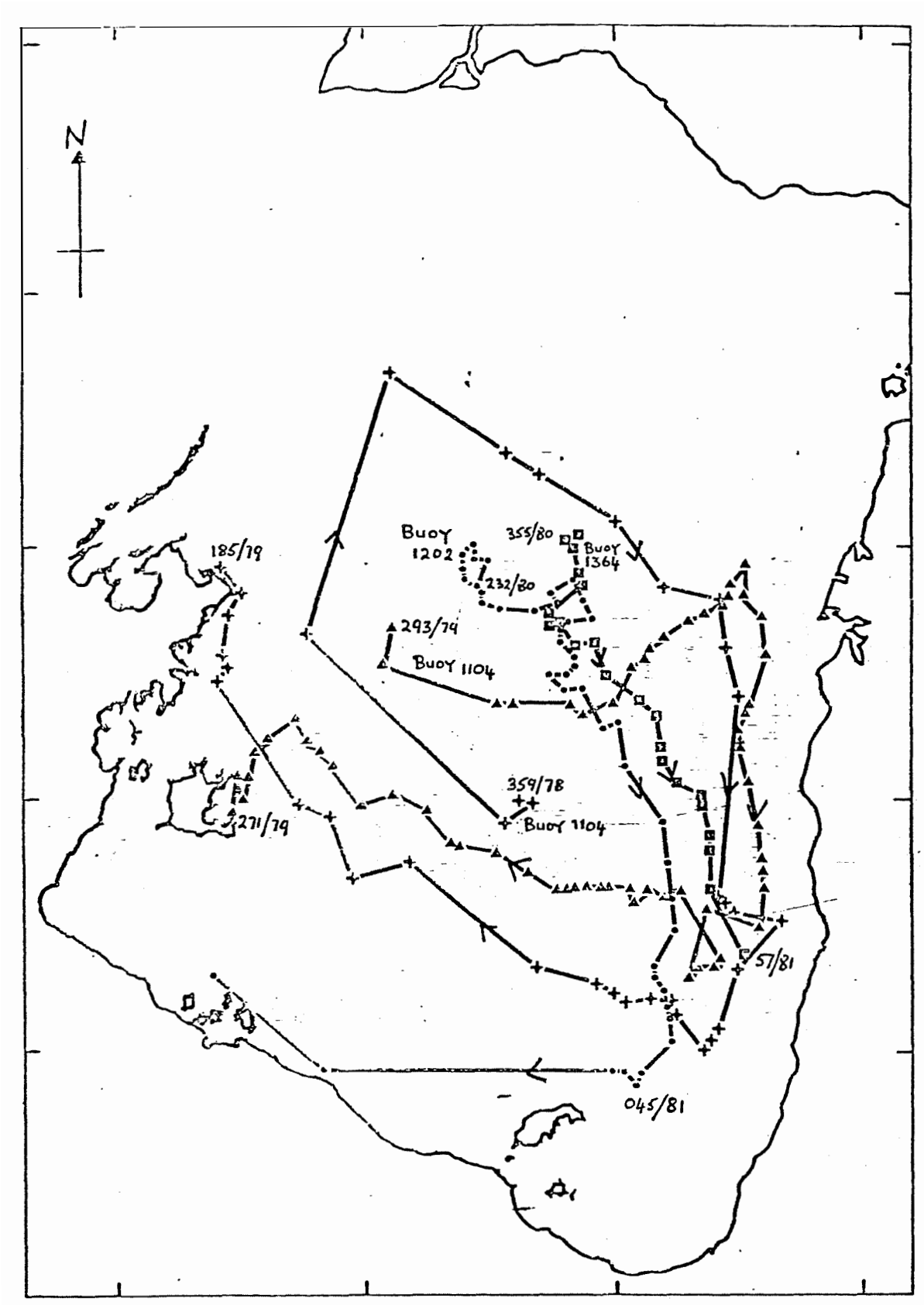

Fig. 9. Satellite-tracked drogued buoy tracks in the Gulf of Carpentaria. Selected day numbers and years are annotated. Buoy 1104 released day 359/1978. Buoy 1104 re-released day 293/1979. Buoy 1202 released day 232/1980. Buoy 1364 released day 355/1980.

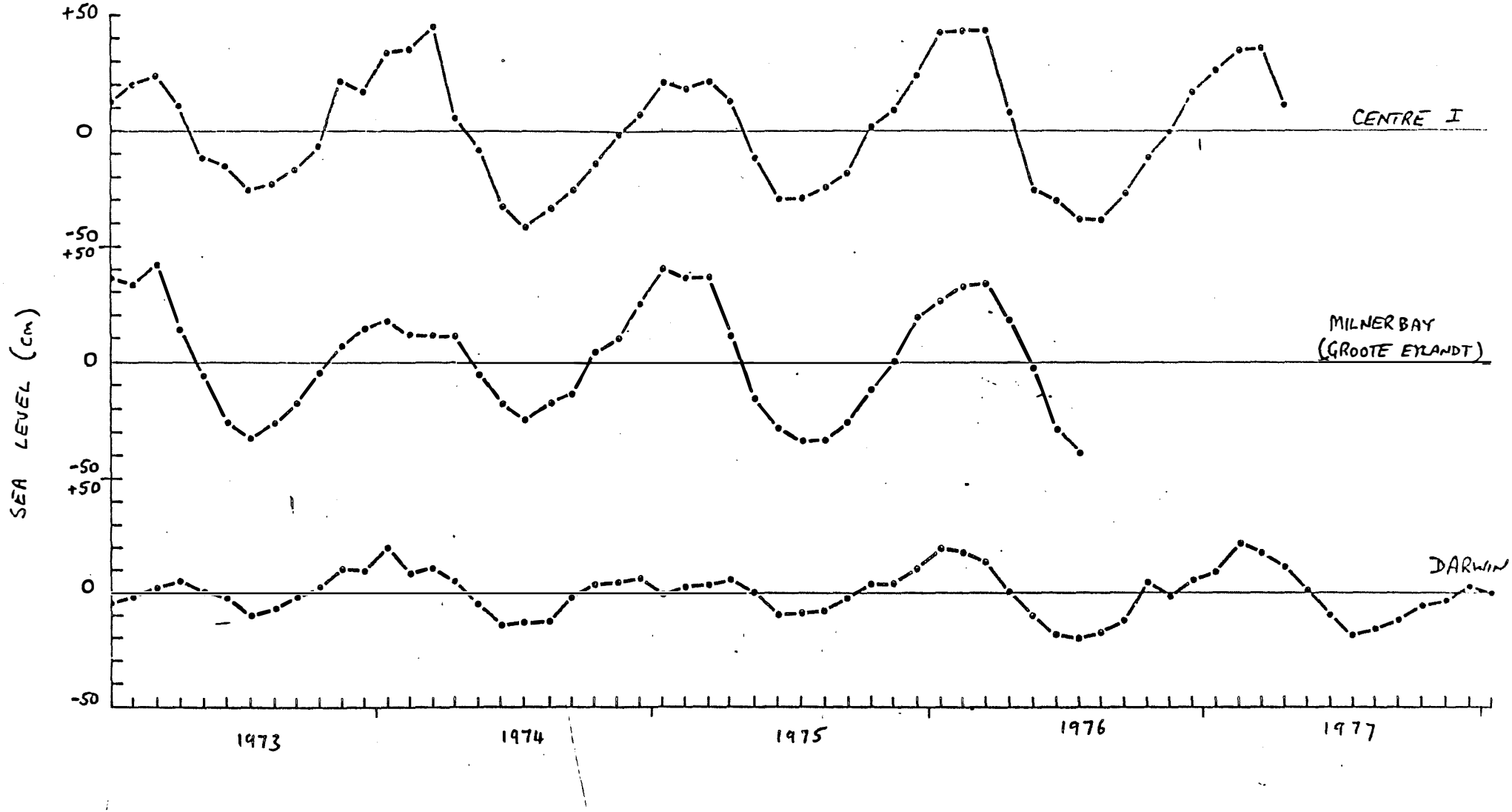

Fig. 10. Monthly mean sea level for Centre Island, Milner Bay and Darwin from 1973 to 1977.

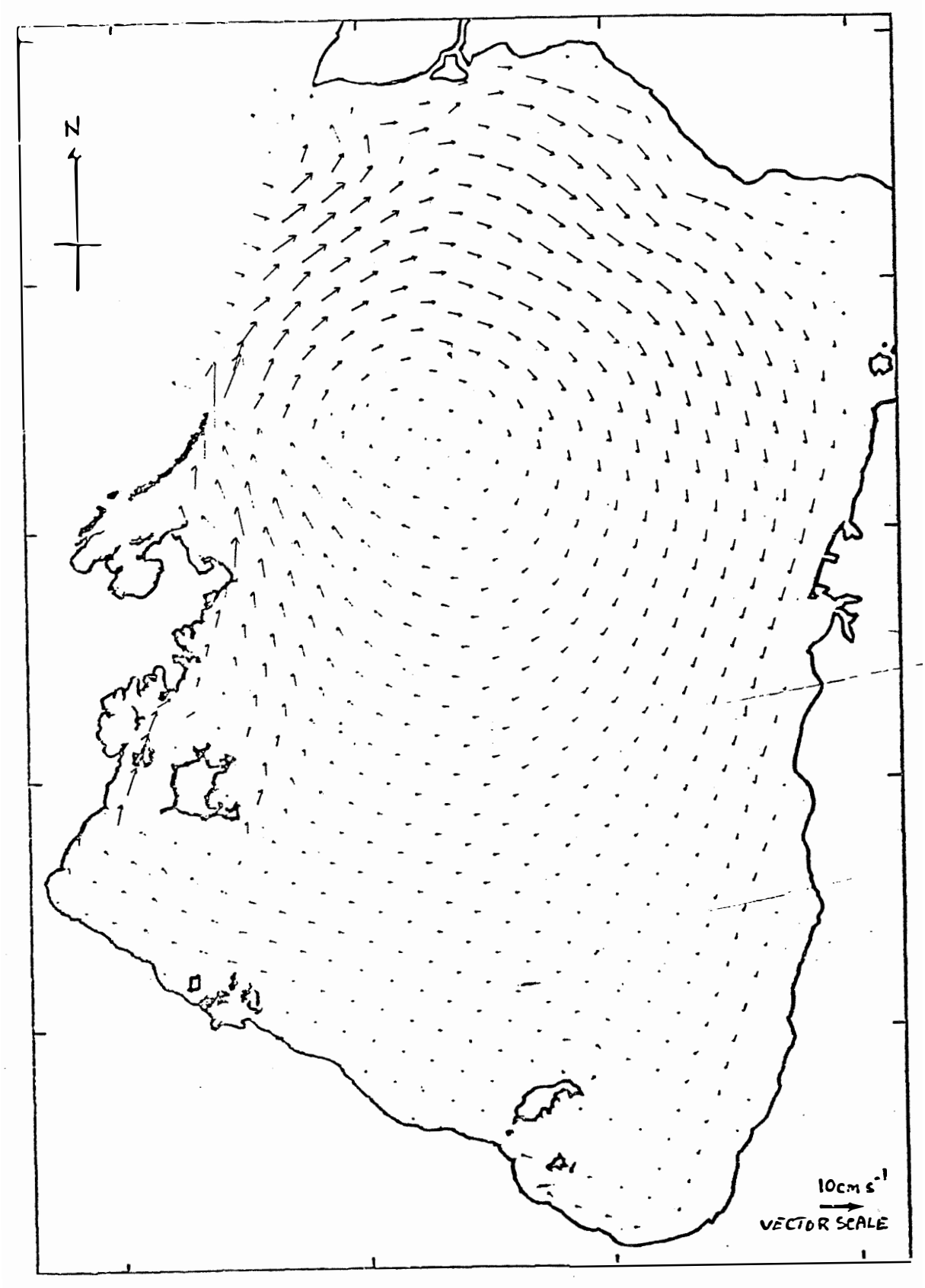

Fig. 11. Residual current vectors on a 15 n mile grid generated from the two-dimensional numerical model of Church and Forbes (1981). This frame shows Lagrangian currents at spring tides.

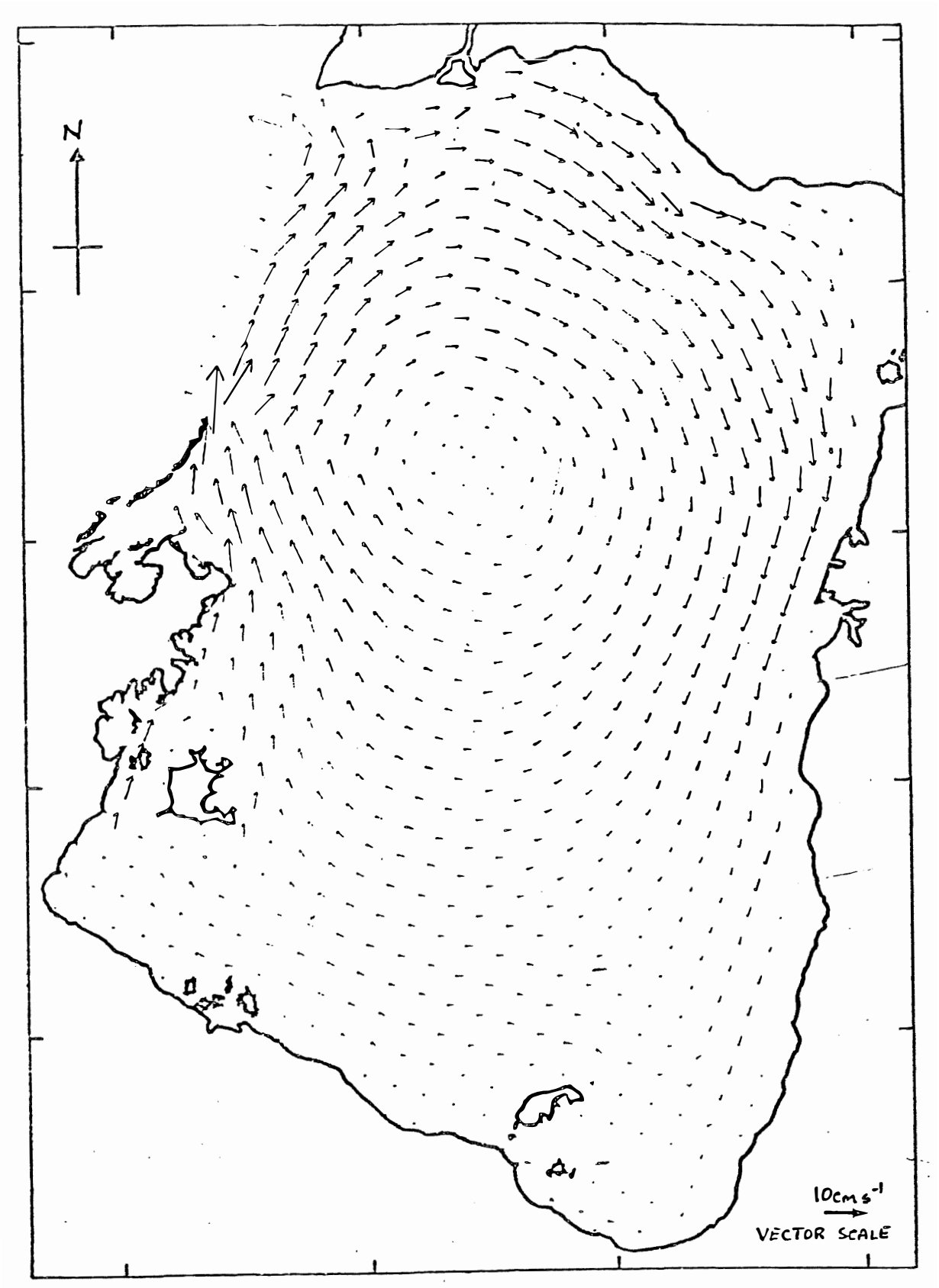

Fig. 12. Residual current vectors at spring tides for January Monsoon wind stress.

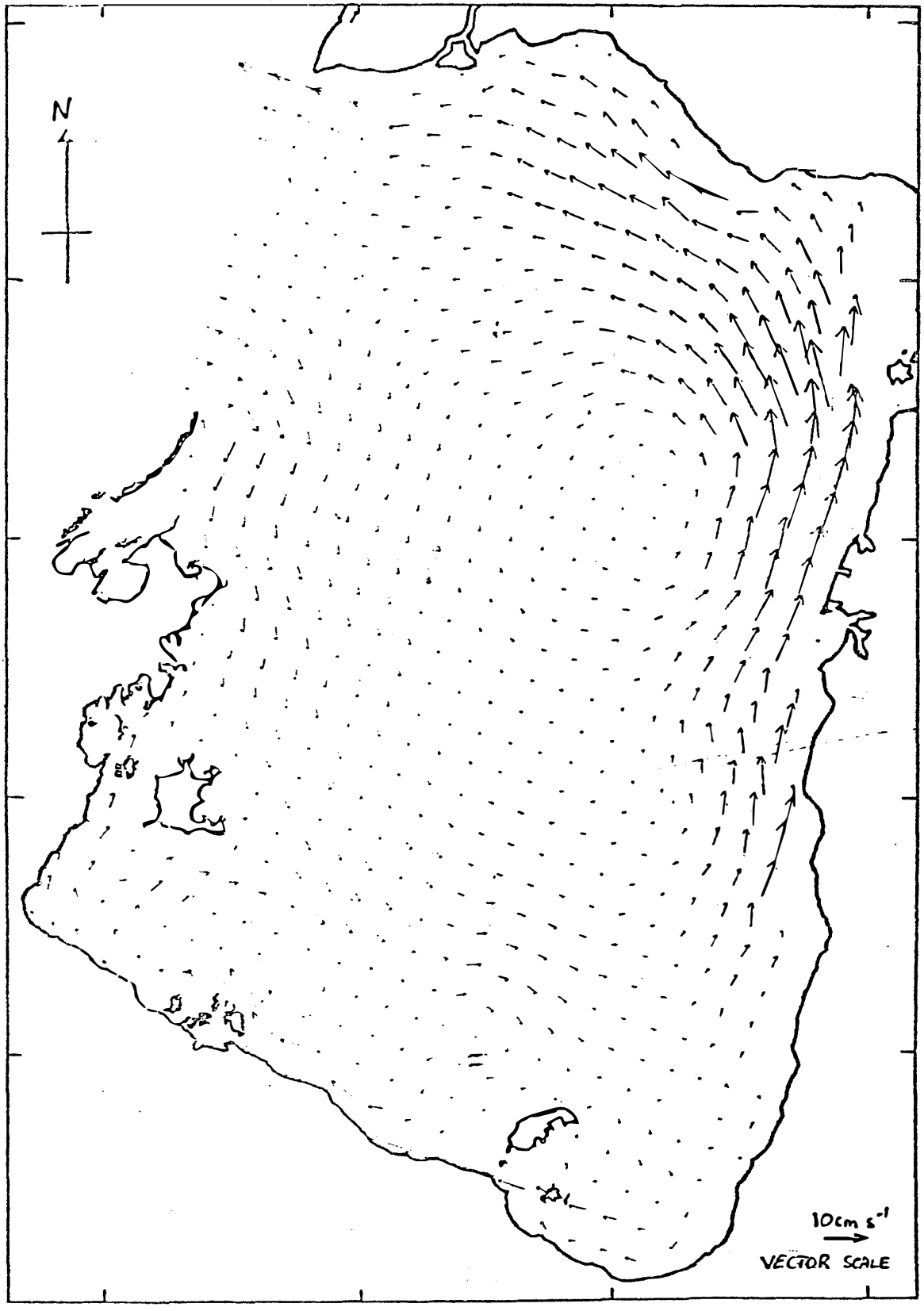

Fig. 13. Residual current vectors at neap tides for July trade wind stress.

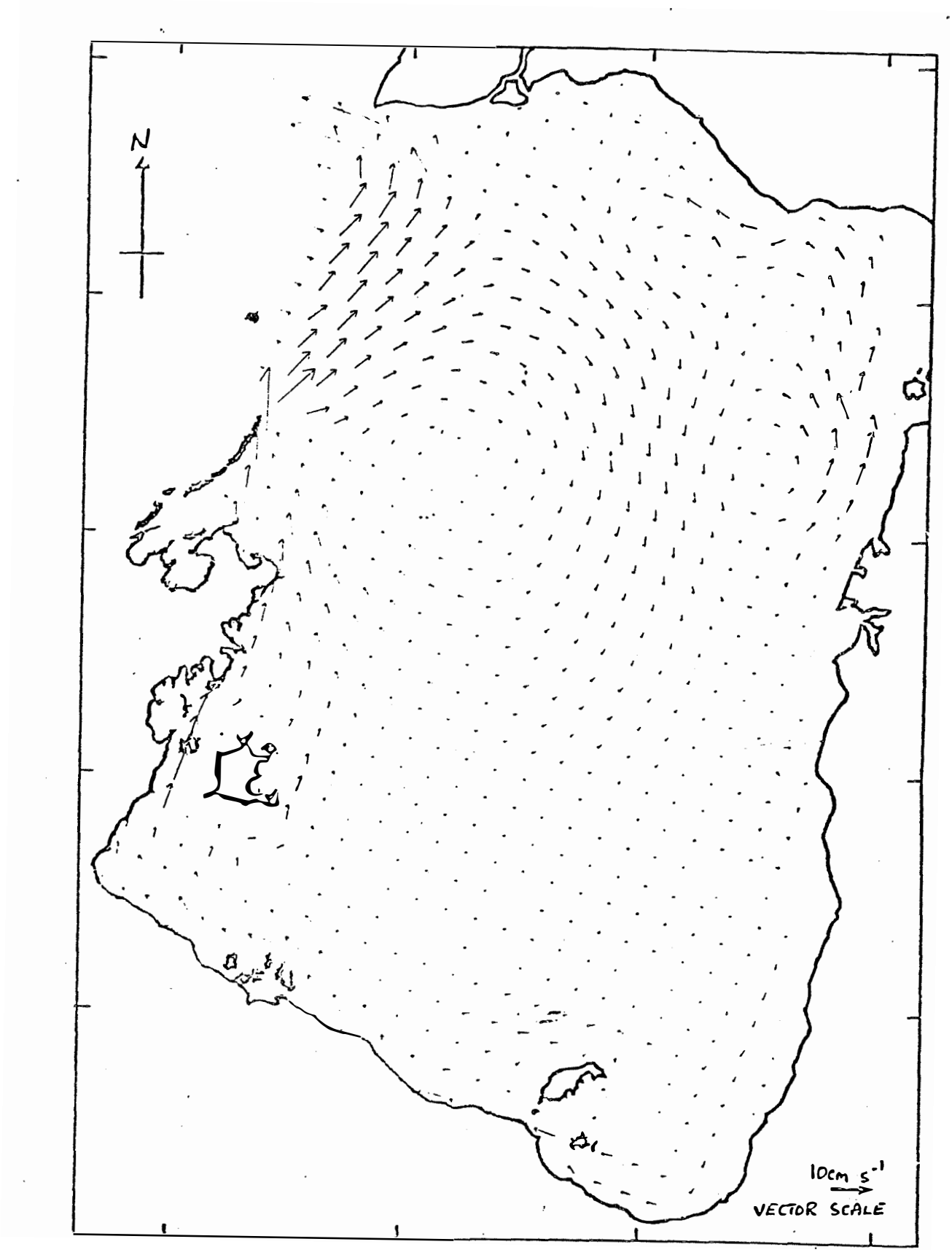

Fig. 14. Residual current vectors at spring tides for July trade wind stress.

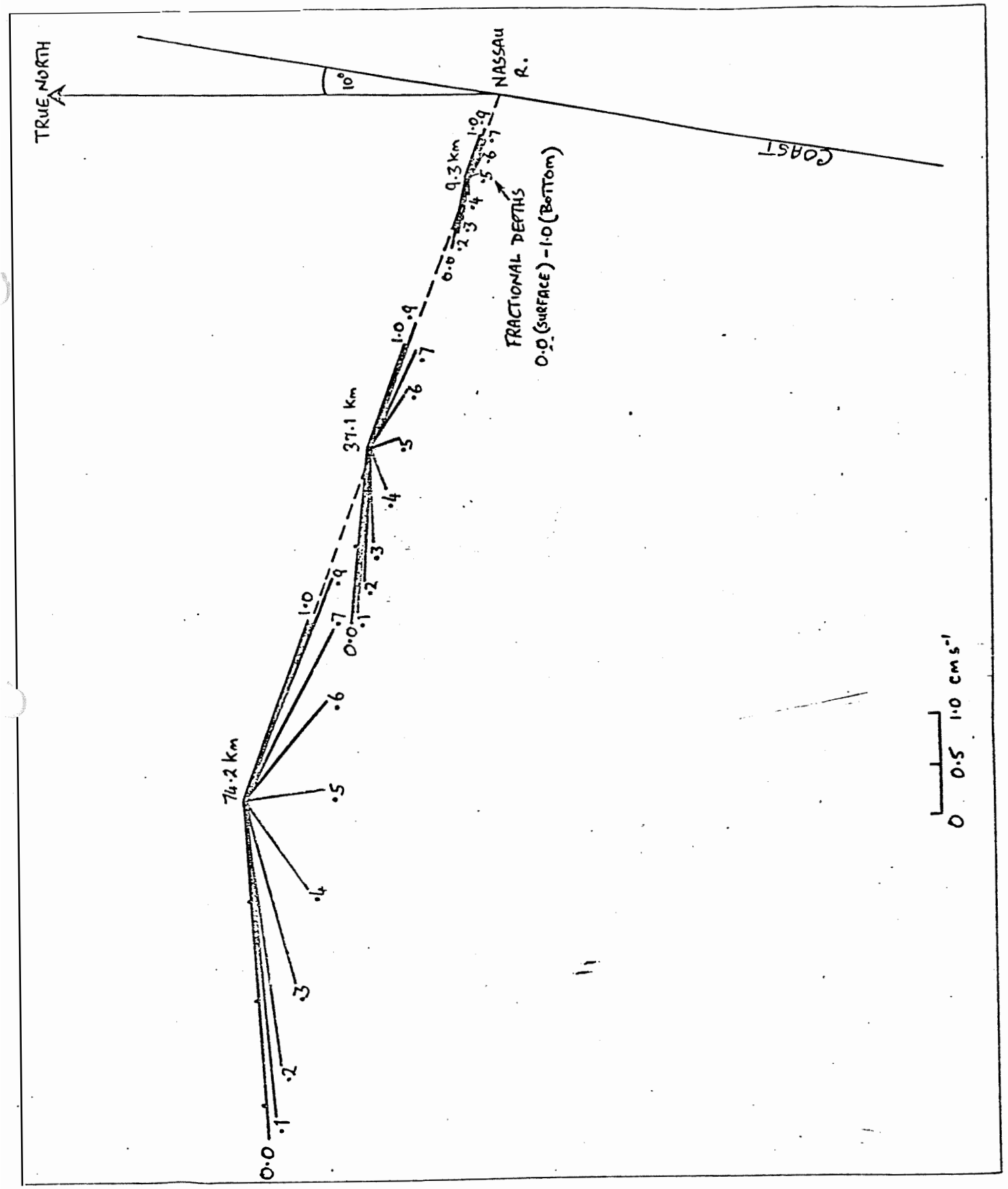

Fig. 15. Plot of density current vectors at selected distances offshore, due to horizontal density gradient, after the method of Heaps (1972). At each location, vectors are plotted at fractional depths as indicated.

78/36

Prediction model for Carpentaria currents developed

by A. M. G. Forbes

In this article Andrew Forbes, a researcher with the CSIRO Division of Oceanography, describes a computer model that predicts tidal and other currents in the Gulf of Carpentaria, originally developed to give a better understanding of banana prawn larvae movements. Earlier results of the research program were published in *Australian Fisheries* in September 1979.

A COMPUTER program that predicts tidal and other currents in the Gulf of Carpentaria has been developed.

This program, or model, was developed initially to provide a better understanding of the movements of banana prawn larvae in the Gulf, but it also gives useful information for navigators.

The study was funded by the Commonwealth Government's Fishing Industry Research Trust Account and conducted by scientists of CSIRO's Marine Laboratories in Cleveland (Brisbane) and Cronulla (Sydney). It involved deployment of six current meters and four satellite-tracked buoys, and the development of the computer model. The model allows the prediction of currents at times and places or under conditions other than those actually measured.

Two different water movements are considered. The first are tidal movements. Although they vary in range, and may be diurnal (once a day) or semi-diurnal (twice a day) in different regions of the Gulf, they are much more obvious than residual currents, the second type considered. These include other intrinsic movements of the sea and also currents caused by wind.

In the short term, tidal currents, being larger, are more important to navigators, but in the long term, the backward and forward movements of the tides tend to cancel each other out and it is the residual currents that largely determine the overall movement.

There had been some earlier oceanographic work on the currents of the Gulf by George Cresswell of the CSIRO Marine Laboratories but for the development of the model more measurements were needed.

Since the basic aim of the study was to understand the movement of banana prawn larvae, and the amount of equipment was limited, current measurements were concentrated in the south-eastern corner of the Gulf, where the majority of the banana prawn catch is taken. These current measurements were later checked against the computer model's predictions.

Current meter measurements

Three pairs of Aanderaa current meters, which measure current speed and direction and sea temperature every 15 minutes and record this information on magnetic tape, were deployed in the southeastern Gulf. (The locations are marked on the map in Figure 1.) One meter was at mid-depth and another near the bottom.

The current meters were serviced and the data tapes collected every six to 10 weeks over a period of six months from September 1978 to March 1979. This length of record means that the tidal currents can be separated by computer processing from the wind driven currents, and the effects of each on the transport of banana prawn larvae assessed.

The results from the bottom meter are similar to those from the top meter at each mooring. Inspection of the example shown in Figure 2 shows that the tide dominates the record, alternating between northward and southward flow once a day. This is called a diurnal tide, and this feature is found in current meter records from all three moorings.

Satellite-tracked buoys

The satellite-tracked buoys are released into the water and transmit their position daily to a satellite, which retransmits the information to a ground station. A 5.4m-diameter parachute attached to the buoy by a weighted 20-m wire ensures that the buoy follows the currents at that depth instead of being blown by the wind.

The first buoy was released in 1978 near the centre of the Gulf (Figure 1) and it made a clockwise circuit of the Gulf in 191 days at an average speed of 0.2 knots. It was re-released in 1979 and again drifted clockwise around the Gulf, this time in 254 days at an average speed of 0.1 knots.

Another buoy released on September 18, 1980 remained almost stationary for 30 days before drifting southeast at a speed of 0.07 knots over 156 days. The last buoy, released on December 20, 1980 drifted parallel

to the previous buoy for 52 days at an average speed of 0.15 knots.

Computer model

It was more convenient to develop a computer model of the circulation in the Gulf than to extend the time and area measured by the current meters. The model is a computer program, which, when given certain initial information, will calculate tide height, and current speed and direction at a grid pattern of points 15 nautical miles apart throughout the Gulf.

Where these points coincide with the position of a current meter or one of the 10 tide stations around the Gulf the model's predictions can be compared with the actual tidal currents measured. If these two do not agree, then the initial information given to the computer is wrong, and a series of small adjustments are made until 'real' and 'computed' measurements are the same.

The initial information required

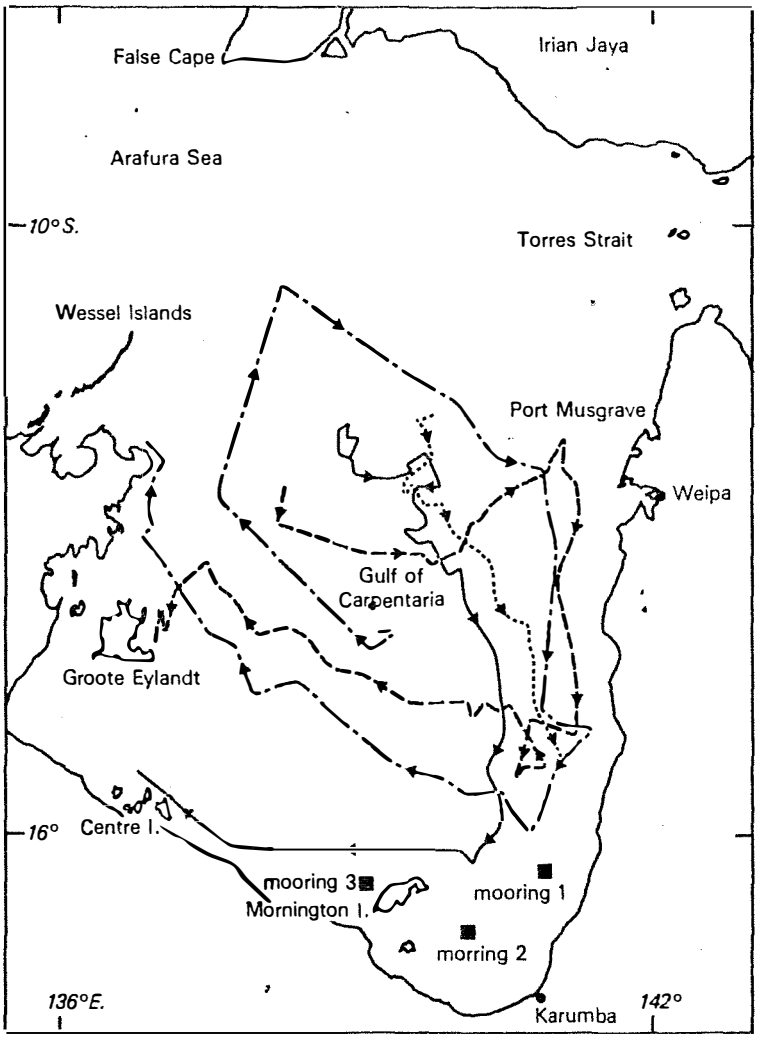

Figure 1. *Positions of the current meter and tracks of the satellite-tracked buoys in the Gulf of Carpentaria.*

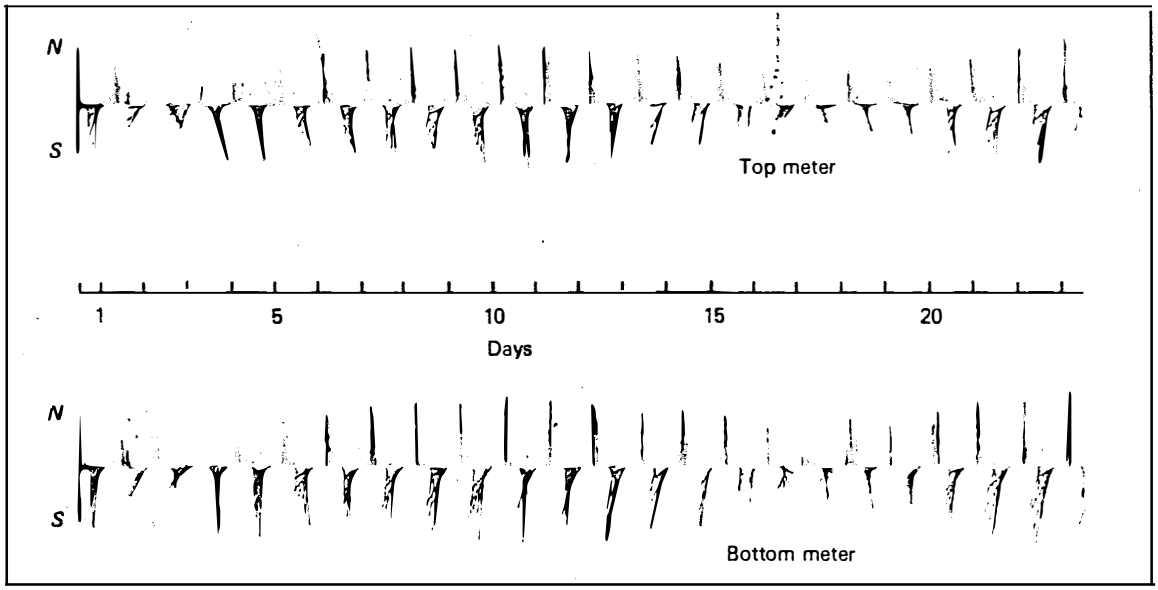

Figure 2. *Example of the record of a pair of current meters. The angle of each 'stick' shows current direction, and its length is proportional to current speed.*

is the tidal height and phase (number of hours before high tide) for a series of points along a line from the Wessell Islands to False Cape in Irian Jaya (West Irian).

The computer calculates the predicted currents and tide heights at each grid point every hour for up to 29 days, a process that takes the computer only a matter of seconds.

Tidal currents

The computer model has several uses, the first of which was to produce a tide stream atlas to aid in understanding the details of tidal currents all over the Gulf. To produce this, the model was run for 25.5 hours to cover a full diurnal tidal cycle and tidal heights and velocities plotted every one-and-a-half hours.

An example of one frame of the model output for spring tides is shown in Figure 3. Tide heights are contoured at intervals of 0.2 m with dashed lines showing height contours lower than mean sea level and solid lines showing contours above mean sea level.

Tidal currents are represented by arrows whose lengths are proportional to current speed. In the top left-hand corner is a speed scale in metres per second and in knots. The set of 16 frames through a diurnal tidal cycle can be used as a tide stream atlas to aid navigation and planning of marine activities. The atlas contains instructions for use and a worked example. (Copies of this atlas are available as Report No. 139, 'Tide Stream Atlas, Gulf of Carpentaria' from: The Librarian, CSIRO Marine Laboratories, PO Box 21, Cronulla, NSW 2230.)

An important, although infrequent, use of the atlas would be in search-and-rescue operations where knowledge is required of the probable tidal trajectory of lost persons or equipment.

Another function of the model is to determine how the diurnal and semi-diurnal tides travel around the Gulf. The northern half of the Gulf is dominated by

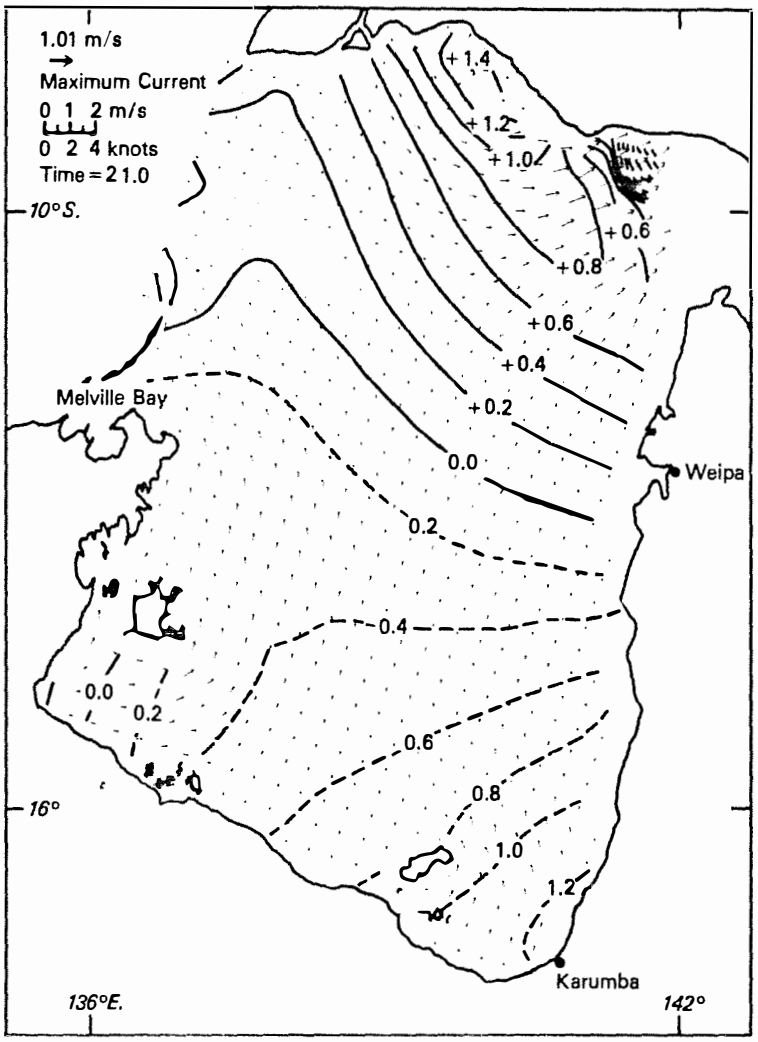

Figure 3. Example of one frame from the Tide Stream Atlas by which the strength and direction of tidal currents in the Gulf of Carpentaria can be measured.

semi-diurnal tides, while the southern half for most of the year has only diurnal tides. The probable explanation for this is that both the semi-diurnal tide and the diurnal tide enter the Gulf as a wave whose crest (which we see as a high tide) travels slowly along the southern coast of Irian Jaya to the north-eastern corner of the Gulf. The geometry of this corner traps the semi-diurnal wave and allows only the diurnal wave to continue to travel southward around the perimeter of the Gulf.

The response of the Gulf to diurnal tides is relatively simple. There is one amphidrome (a region of very small tides) near the centre of the Gulf, and the tide rotates clockwise around this point.

For the semi-diurnal tide, there are two amphidromes about which the semi-diurnal tide rotates clockwise, one northwest of Mornington Island and another southeast of Groote Eylandt, and a region of small tidal amplitude up the middle of the Gulf from Mornington Island to Merauke (in Irian Jaya).

Residual currents

The model was used to simulate residual currents (which are the

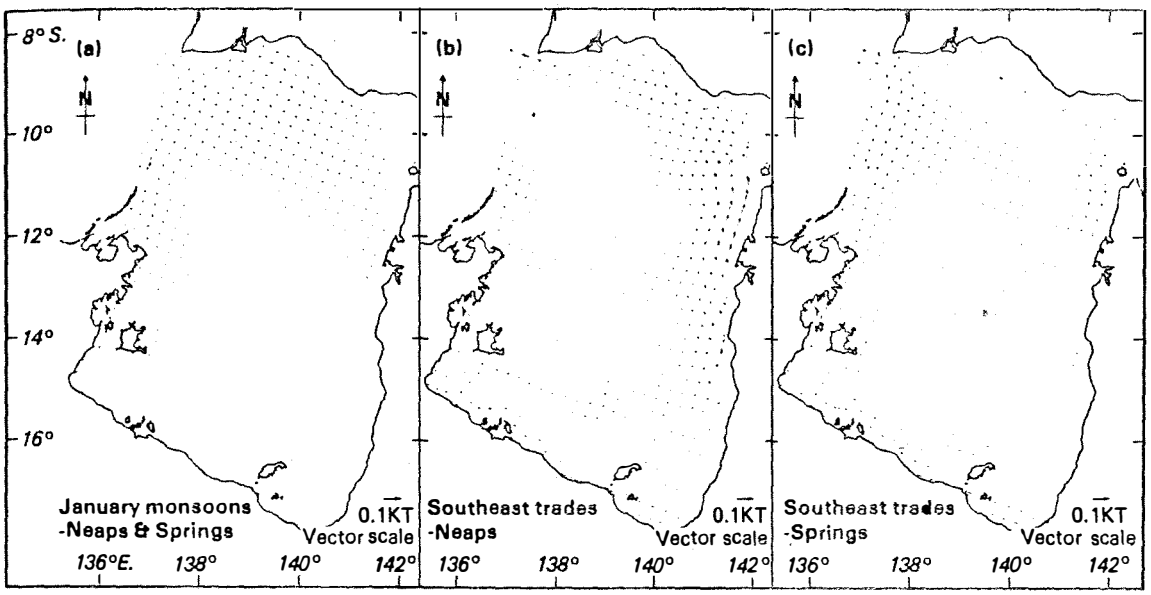

Figure 4. Examples of the residual currents predicted by the computer at different seasons and tides.

small currents left after averaging out the strong flood and ebb currents). These are clockwise round the Gulf at about 0.1 knot for spring tides (although in some areas currents are as strong as 0.2 knot) and 0.02 knot for neaps, which compares well with observations of satellite-tracked buoys (Figure 1).

The model was re-run for spring and neap tides taking into account the January monsoon wind. The effect of the north-west monsoon is to enhance the weak clockwise tidal residual currents. For both spring and neap tides, the wind-driven clockwise currents are typically 0.1 knot in the north, 0.15 knot in the east and 0.2 knot on the western side (Figure 4a). Residual currents in the south-eastern corner are approximately 0.02 knot, showing that the weaker wind in that region produces very little current.

Under the influence of the south-east trades, the model's weak clockwise residual currents at neap tides are reversed in the northern half of the Gulf (Figure 4b) creating an anticlockwise gyre centered at 12 °S, 140 °E. A strong northerly flow along the eastern side of the Gulf characterises this circulation. Below 15 °S, there is a slow clockwise circulation, typically 0.1 knot, centred 55 km northeast of Centre Island.

During springs (Figure 4c) the tidal residual currents are stronger, so the trade winds make a smaller contribution to the flow. The clockwise tidal residual currents are reduced to about 0.05 knot and a smaller anticlockwise gyre with maximum currents of 0.2 knot is generated in the north-east, centred off Port Musgrave.

Prawn larvae movement

The third and most important purpose for developing the model was to test possible mechanisms of banana prawn larval transport from various spawning locations to river estuaries at different times of the year.

Since the model and observations show that tidal currents at a point in the coastal zone oscillate back and forth, with flood tide in the opposite direction to ebb tide, it is clear that the degree of inequality of the two tidal flows (the residual tidal current) is important in establishing a net movement of larvae.

If the flood tide is southward and stronger than the northward ebb flow, for example, then over a diurnal tidal cycle (25 hours) prawn larvae would be carried gradually southwards.

To determine this net transport, the tidal model was run for two-week periods, including realistic winds in October and March. These results show that the net transport of larvae in the south-east corner would be coastward during the October spawning and offshore during the March spawning. This clearly has an important influence on the survival of the prawn larvae, for those which do not reach the shallow coastal regions will perish.

The results of applying the model to the movement of prawn larvae will be the subject of another article.

Solar refrigeration research grant

A GRANT of $154 660 has been made to Wildridge and Sinclair Pty Ltd and the University of Sydney to demonstrate the use of solar-powered refrigeration for fish storage.

It was one of 116 energy research and development grants having a total value of almost $16.7 million announced last month by the Minister for National Development and Energy, Senator Sir John Carrick.